T.R.
GEBZE TECHNICAL UNIVERSITY
GRADUATE SCHOOL OF NATURAL AND APPLIED SCIENCES

S BAND VIRCATOR DESIGN, SIMULATIONS AND MEASUREMENTS

HASAN ERCİYAS
A THESIS SUBMITTED FOR THE DEGREE OF
MASTER OF SCIENCE
DEPARTMENT OF PHYSICS
METROLOGY PROGRAMME

GEBZE
2019

T.R.

GEBZE TECHNICAL UNIVERSITY

GRADUATE SCHOOL OF NATURAL AND APPLIED SCIENCES

S BAND VIRCATOR DESIGN, SIMULATIONS AND MEASUREMENTS

HASAN ERCİYAS

A THESIS SUBMITTED FOR THE DEGREE OF

MASTER OF SCIENCE

DEPARTMENT OF PHYSICS

METROLOGY PROGRAMME

THESIS SUPERVISOR

PROF. DR. BULAT RAMİ

GEBZE

2019

T.C.
GEBZE TEKNİK ÜNİVERSİTESİ
FEN BİLİMLERİ ENSTİTÜSÜ

S BAND VİRKATÖR TASARIMI, SİMÜLASYONLARI VE ÖLÇÜMÜ

HASAN ERCİYAS

YÜKSEK LİSANS TEZİ
FİZİK ANABİLİM DALI
METROLOJİ PROGRAMI

DANIŞMANI
PROF. DR. BULAT RAMİ

GEBZE
2019

GEBZE TEKNİK ÜNİVERSİTESİ	**YÜKSEK LİSANS JÜRİ ONAY FORMU**

GTÜ Fen Bilimleri Enstitüsü Yönetim Kurulu'nun 24/04/2019 tarih ve 2019/20 sayılı kararıyla oluşturulan jüri tarafından 10/05/2019 tarihinde tez savunma sınavı yapılan Hasan ERCİYAS 'ın tez çalışması Fizik Anabilim Dalı Metroloji Programında YÜKSEK LİSANS tezi olarak kabul edilmiştir.

JÜRİ

ÜYE
(TEZ DANIŞMANI) : Prof. Dr. Bulat RAMİ

ÜYE : Dr. Öğr. Üyesi Bektaş ÇOLAK

ÜYE : Doç Dr. Fikret YILDIZ

ONAY

Gebze Teknik Üniversitesi Fen Bilimleri Enstitüsü Yönetim Kurulu'nun

...../...../..... tarih ve ...../..... sayılı kararı.

SUMMARY

In this study, virtual cathode oscillator (vircator) design, modeling and measurement studies are discussed. The frequency band for the designed and measured vircator model is 2-4 GHz. CST Particle Studio and MATLAB programs were used for design studies. When using MATLAB for mathematical modeling, CST Studio was evaluated for simulation and analysis. For the stimulation of the vircator cathode, a Marx Generator, capable of producing 400kV and 600 ns pulses, was used. In this study the vircator was produced in accordance with the output impedance of the Marx Generator connected to the output of the Marx generator to take measurements. The measurements were performed in 3 different ways. In the first scenario, the microwave signal from the output of the vircator was measured with a wide band horn antenna. In the second scenario, measurements were performed using the d-dot probe. In the last scenario, the output power was calculated by using the horn antenna and microwave power measurement sensor together. The results were compared with the results of the simulation program and the results were evaluated.

Key Words: Virtual Cathode Oscillator (VİRKATÖR), Microwave Signal (MS), CST Particle Studio (CST PS).

ÖZET

Bu çalışmada bir mikrodalga üreteci olan sanal katot osilatörü (virkatör) tasarımı, modellenmesi ve ölçüm çalışmaları ele alınmıştır. Tasarlanıp ölçülen virkatör modeli için frekans bandı 2-4 GHz olarak şeçilmiştir. Tasarım çalışmaları için CST Particle Studio ve MATLAB programları kullanılmıştır. Matematiksel modelleme yapılırken MATLAB kullanılırken, benzetim ve analiz için CST Studio değerlendirilmiştir. Virkatör katodunun uyarılması için 400kV maksimum voltaj ve 600 ns darbe genişliği üretebilen Marx Jeneratörü kullanılmıştır. Marx Jeneratörünün çıkış empedansına uygun olarak üretilen virkatör, Marx jeneratörünün çıkışına bağlanarak ölçümler alınmıştır. Ölçümler 3 farklı şekilde gerçekleştirilmiştir. Birinci senaryoda virkatörün çıkışından alınan mikrodalga sinyali geniş band horn anten ile ölçülmüştür. İkinci senaryoda ise d-dot probe kullanılarak ölçümler gerçekleştirilmiştir. Son senaryoda ise horn anten ve mikrodalga güç ölçme sensörü birlikte kullanılarak çıkış gücü hesaplanmıştır. Ölçüm sonuçları benzetim programı ile yapılan analizler ile karşılaştırılarak sonuçlar değerlendirilmiştir.

Anahtar Kelimeler: Sanal Katot Osilatörü (VİRKATÖR), Mikrodalga Sinyal (MS).

ACKNOWLEDGEMENTS

I am greatly thankful to my thesis advisor Prof. Dr. Bulat RAMİ for his invaluable contributions and support through my graduate period of time. Additionally, I would like to thank Prof. Dr. Ahmet Arif ERGİN who support me to start my profession and contributed a lot to me, also I would like to express my gratitude to Kadir DURGUT who has been with me since the day I started my career, my best friend Ömer FARUK KİP who is always with me during my studies, my valuable co-workers included in KAMTAM team especially Feyzullah YAYIL, Dr. Selahattin NESİL, Emirhan POSTACI and Nergis Yıldız ANGIN ATMACA who motivate me during my works and support me for my thesis studies as well. I would like to add my sincere thanks to my mother Halime ERCİYAS, my father Durak ERCİYAS, my brother Harun ERCİYAS for whom I felt their love and support throughout my life and I would like to thank my dear wife Yonca ERCİYAS for her everlasting support.

TABLE of CONTENTS

LIST of ABBREVIATIONS and ACRONYMS

Abbreviations and Acronyms		**Explanations**
Vircator	:	Virtual Cathode Oscillator
HPM	:	High Power Microwave
CST-PS	:	Computer Simulation Technology- Particle Studio
I_b	:	Electron Base Current (A)
I_{SCL}	:	Space Charge Limited Current (A)
R	:	Radius of Cavity (m)
r_0	:	Cathode Radius (m)
c	:	Speed of Light (m/s)
ρ	:	Electron Density
e	:	Electron Charge
m	:	Electron Mass
γ	:	Relativistic Factor
D	:	Anode-Cathode Distance
V	:	Voltage
v	:	Speed of Electron
J_{SCL}	:	Space Charge Density
ε_0	:	Permeability of Free Space
Φ(z)	:	Potential in Free Space
λ	:	Wavelength
λ_{wg}	:	Wavelength in Waveguide
P	:	Diode Permeability
P_{CL}	:	Cathode Perveance
I	:	Current (A)
f_p	:	Plasma Frequency
f_{vc}	:	Virtual Cathode Oscillation Frequency
PFL	:	Pulse Forming Line
CsI	:	Cesium Iodide

LIST of FIGURES

LIST of TABLES

1. INTRODUCTION

1.1. Vircator Overview

Vircators are the systems that can produce short pulse duration microwaves. Generated waves can rise to very high power levels and the system makes it possible to obtain high power microwaves with Marx generators usage. A proper vacuum tube that is used to convert these high energy pulses into microwaves is called as vircator.

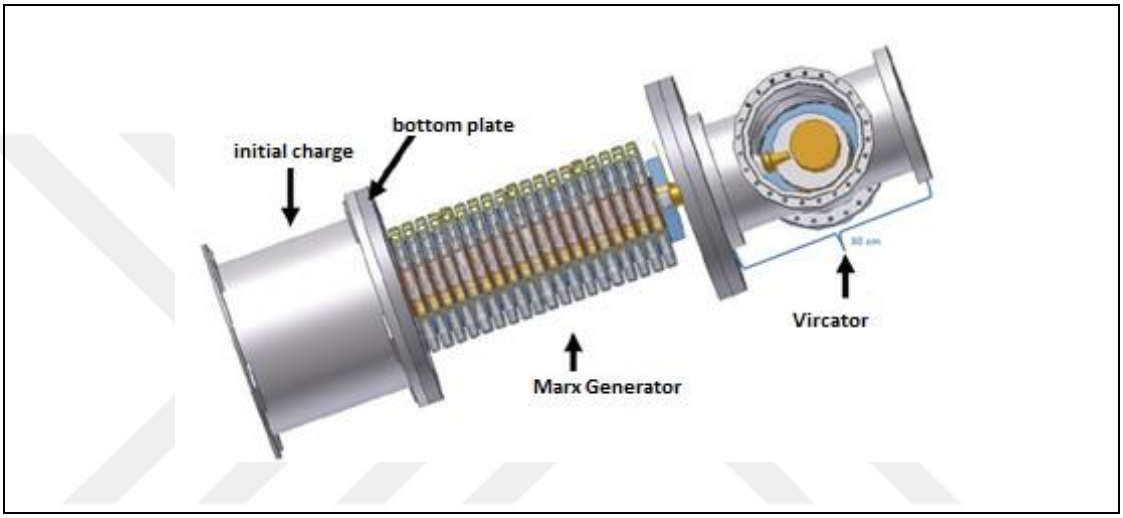

Figure 1.1: General view of vircator.

Vircator is a microwave generator which doesn't need an external magnetic field. Its main working principle is based on the equivalence of the oscillation frequency and plasma frequency of relativistic electron beam. Vircator operating frequency ranges between 300 MHz-40 GHz, however its efficiency is lower relative to other kinds of high power microwave generators. They are mostly preferable due to their simple structure, lower production cost, adjustable frequency option, wide bandwidth and capability of producing powers of gigawatt levels in a short duration pulses such as 100ns or lower. Vircators are also single shot devices that can operate at large bandwidth. That is why they are used more common with respect to other high power microwave generators.

In addition to the simple mechanical structure of vircator, they are frequently preferred in systems which require high power microwave due to their durability and

small size. While low frequency generating vircators are used for electronic interference, high frequency generating devices are used to destroy electronic devices.

To sum up; vircator is a microwave generator which stops lots of electronic devices (especially devices which communicate via radio waves by using long cables) for a short period of time or permanently via producing high amplitude electromagnetic pulses. In other words, vircator is a microwave generator that is used in the purpose of destroying electronic components.

1.2. Contribution and Aim of the Thesis

The production of high power microwaves which have been on the agenda in recent years and had been reaserched intensely is an important issue in terms of especially for the defense systems of country as well as the directing this electromagnetic waves to a target at desired distance.

The term electromagnetic defense can be defined as the use of directed electromagnetic energy for the purpose of preventing or counter attacks. Vircator is a generator that can be used in this context and it can be produced simpler relative to other generators.

Directed electromagnetic energy term is based on two fundamental concepts. In the first concept, the objects are tried to be thrown away via HPM. For the second application, HPM pulses are directly sent or microwaves are sent to the target.

This thesis focuses on the vircators among the other kind of HPM generators. In this context, vircator theory, characteristic features, classification and system elements are considered under the main title of vircator theory.

In the second part of the thesis, the production of a vircator prototype in laboratory environment, determination of frequency and electric field strength, attenuation of signal depending on the distance and the effect on different electronic devices are examined.

2. VIRCATOR THEORY

The researches on vircator started in the 1960's. The standard vircators which have cathodes fed by negative pulses and anodes having ground potential were becoming popular in the 1980's. Virtode or feedback vircator was first studied at Kharkov Physics Technical Institute in 1993 and coaxial vircator was first studied as computer simulation at Texas Technical University in 1997.

Vircators differ from other sources of HPM in the production of electromagnetic radiation. For traditional HPM sources, while electromagnetic radiation is produced via interaction between the electron beam and cavity, electrons are accelerated from cathode to the anode in the vircator systems. Vircator anode is transparent to the electron beam and they pass through this anode when their potential energy is greater than kinetic energy (when reaching the space charge limiting current). After they pass to the other side of this transparent anode, they formed an electron beam cloud which is named as virtual cathode. This electron cloud oscillates and the electrons oscillate between the cathode and virtual cathode as well. In this way, microwave radiation is produced.

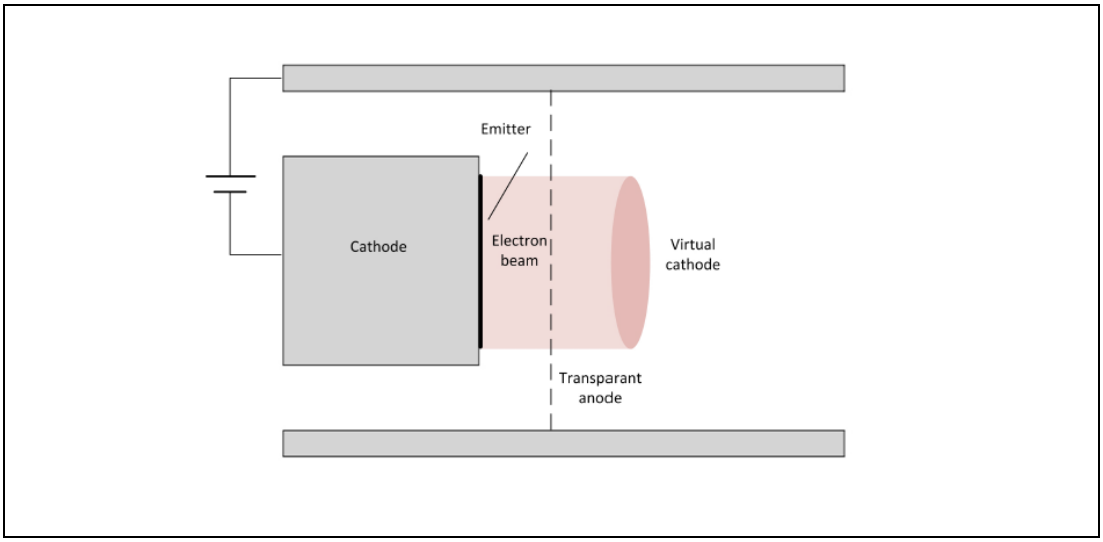

Figure 2.1: Vircator structure.

HPM sources such as vircators need high voltage and current. Generator source performance strongly depends on the structure of material used for electrodes.

Appropriate emitter materials used for vircator cathodes can be listed as velvet, carbon fiber, aluminum, steel and copper.

Dielectric materials such as velvet emits electrons via explosive emission field mechanism. This electron emission is based on the plasma formation within the fibers however in the case of excessive plasma creation, vacuum level decreases which results in the performance deterioration. In order to make the velvet stick together with the cathode metal base, electrically conductive and high temperature resistant adhesives can be used. Since it is applied a very high voltage in between the anode – cathode gap, it is allowed to emit electrons from velvet micro fibers thanks to the highest electric field value takes place at the fiber tips.

The main working principle of the vircator is acceleration of the intense electron beam to the anode with gridded or meshed structure. When the electron beam with base current I_b exceeds space charge limited current I_{SCL}, majority of electrons pass through the anode and form the electron cloud called as virtual cathode. Virtual cathode parameters having the feature of adjustibility, determine the mode of resonance in which the microwave oscillates. It can be changed the operating frequency of virtual cathode by adjusting the density of virtual cathode without the need of external magnetic field. Space charge limited current I_{SCL} needed for the formation of virtual cathode in the cylindrical vacuum tube geometry can be obtained by taking into account the formula below. This relation is known as Child – Langmuir equation.

$$I_{SCL} = \left(\frac{mc^3}{e}\right)\frac{\left(\gamma^{\frac{2}{3}}-1\right)^{\frac{3}{2}}}{1+2ln\left(\frac{R}{r_0}\right)} \quad \left(\frac{mc^3}{e} = 17kA\right) \tag{2.1}$$

Here R is the radius of the cavity, r_0 is cathode radius, c is speed of light, e is electron charge and m is the mass of electron. γ is the relativistic factor of electron beam at the anode and it can be obtained from the equation below.

$$\gamma = 1 + \frac{Voltage(kV)}{511} \tag{2.2}$$

Vircators operate at narrow bandwidth, however they can be designed to make them generate HPM having frequency range between ~0.5 – 40 GHz according to their structural dimensions. Their output power can span in between 1 MW and 20 GW. Vircator tubes are in vacuum in order to produce microwave power.

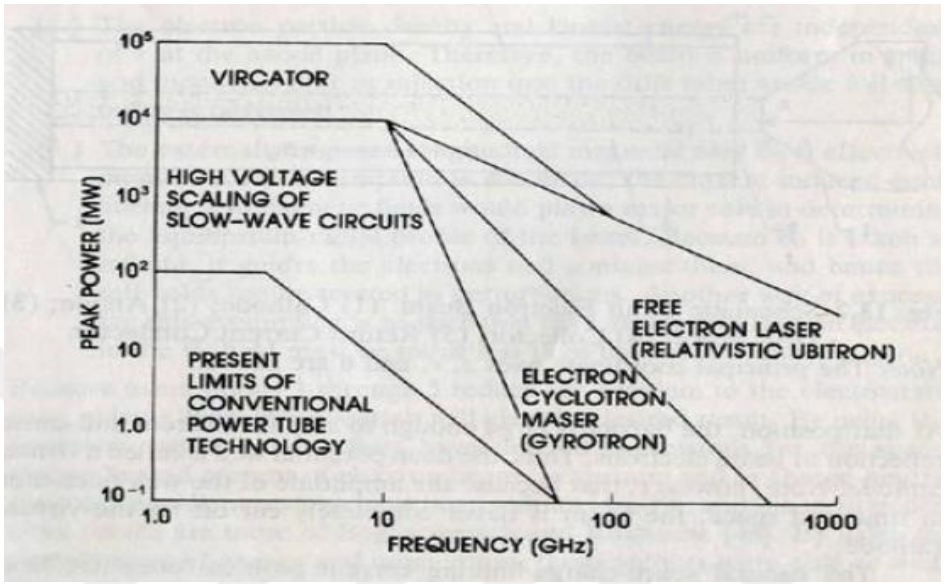

Figure 2.2: High Power Microwave Sources.

2.1. Space Charge Limited Current

It is calculated space charge limited current rather than total current if it is imagined that the cathode and anode have infinite lengths. In this calculation the distance between anode and cathode is taken as D and the voltage is V.

(2.3)

The parameters ρ and v, refers to the functions of the distance z between the two plates. They express electron density and velocity respectively. Since the electrons are only originated from the cathode, they only flow when the anode is positive with respect to the cathode. It is assumed that the diode is infinite in x and y dimensions, therefore these components are ignored and the all of the vectors are taken as scalar. According to the conservation of charges, J_{SCL} doesn't change with z

and for this reason it takes a constant value between the anode and cathode. Since it is dealt with only the electron density from cathode to the anode in positive z direction, it is convenient to put a minus sign conventionally. It can be calculated v(z) according to the energy conservation:

$$-\qquad\qquad)=\text{sabit}=0 \tag{2.4}$$

(z) is the potential field meanwhile m and e are electron mass and charge respectively. For simpler calculation total energy is taken as zero (for the electrons left in the cathode which is grounded at the beginning). The potential ϕ(z) must verify Poisson equation.

$$\frac{}{} \tag{2.5}$$

ε is the permittivity of a free space. If $\rho(z)\ and\ v(z)$ cancel each other, by using the equations it is obtained a second order non – linear differential equation for the potential:

$$\frac{}{} \quad \frac{}{\sqrt{\frac{}{}}\sqrt{\phi}} \tag{2.6}$$

If it is multiplied with $\frac{}{}$ both sides [38],[39]:

$$\left(\frac{}{}\right) \quad \frac{}{}\sqrt{\frac{}{}}\sqrt{\phi}$$

$$\frac{}{}\sqrt{\frac{}{}}\sqrt{\phi} \quad \left(\frac{}{}\right) \tag{2.7}$$

K constant can be found by applying boundary conditions, $\phi(0) = 0$. Negative derivative of potential gives the electric field magnitude. Therefore, K is the square of the electric field magnitude at the cathode surface.

If there were no electrons in the anode – cathode region, the electric field magnitude at the cathode would be simply V/D in the direction of electron acceleration from cathode to the anode. While the electrons enter to the free space, they change the electric field due to their charges itself. Migrating a large number of electrons in to this region makes the electric field at cathode surface to be zero and prevents more electrons from acceleration. Zero electric field approach at the cathode surface is a must for the space charge limited emission. Any addition of electron ejection causes to electric field to be reversed and electrons to be accelerated towards the cathode. In a stable state, the electrons collected on the anode leave the anode cathode gap, in this way there are more electrons enter to this region. This process increase the space charge limited current density.

Space charge limited field potential can be found by taking the integral of square of the equation with the zero electric field assumption on the cathode:

$$\phi(z) = \left(\frac{3}{2}\right)^{4/3} \left(\frac{J_{SCL}}{\varepsilon_0}\right)^{2/3} \left(\frac{m}{2e}\right)^{1/3} z^{4/3} + K \tag{2.8}$$

If integration constant is taken as zero for the $\phi(0) = 0$ boundary condition and anode potential is determined as $\phi(D) = V$, the equation can be solved for space charge limited current density:

$$J_{SCL} = \frac{4}{9}\varepsilon_0 \sqrt{\frac{2e}{m}} \frac{V^{3/2}}{D^2} \tag{2.9}$$

2.2. Space Charge Limited Emission

Ionized gas clouds created by explosive emission mechanism, consist of lots of electron emission sources. Applied electric field causes to the field limited electron flow from each of the ionized gas clouds. If the applied voltage V_d does not exceed a few hundreds of kV, electron current emitted from plasma resembles Child-Langmuir $I = PV_d^{3/2}$ formulation [38],[39]. Diode perveance P only depends on the diode geometry.

2.3. Cold Cathode Explosive Emission

Electron emission utilized in the vircator systems is obtained by applying a very high voltage to the anode and cathode gap. Electrons are emitted from cathode by applying hundreds of kV's to the cathode. Emission process in the cold cathode is explained by the explosive emission mechanism. Almost all metal cathode surfaces have microscopic protrusions either from the material itself or from the production. When high voltage is applied to the cathode surface, the electric fields formed on these small protrusions rise to much high levels, causing evaporation. This evaporation expands and fuses on the cathode surface. The plasma created on the cathode surface becomes an infinite electron source. Electron source can produce a current density of tens of kA/cm^2. In other words, for the explosive emission mechanism, cathode surface plasma is an electron source rather than cathode itself. Another different plasma formation takes place at the anode during the microwave output of the vircator. As electrons emitted from the cathode plasma pass through the transparent anode, some strike the anode and cause the anode temperature to rise. Created anode plasma emits ions from anode to the cathode. This process is called as bipolar flow.

2.4. Frequency Characteristic of Virtual Cathode

The virtual cathode is formed at the other side of the anode, when the current between the anode and cathode I_b exceeds the space charge limited current value. Two things occur when the virtual cathode is formed: (1) virtual cathode oscillates back and forth at the beam plasma frequency (ω) (2) while some of the electrons travel along the virtual cathode, some of them reflects towards the cathode. Reflected electrons return back from the cathode potential and enter the virtual cathode region. Virtual cathode oscillation occurs mostly at different frequency from the reflex frequency, however vircator operation can be adjusted for these two frequencies to overlap [38], [39]. I_{SCL} current can be expressed by equation below;

$$I_{SCL}(kA) = \frac{8.5}{G}(\gamma_0^{2/3} - 1)^{3/2} \tag{2.10}$$

The electron beam voltage V_0 between anode and cathode,

$$\gamma_0 = 1 + \frac{eV_0}{mc^2} = 1 + \frac{V_0(MV)}{0.511} \tag{2.11}$$

and G depends on geometry. For example, for a ring shaped electron beam with radius r_b in a cylindrical vacuum tube having radius r_0,

$$G = ln\frac{r_0}{r_b} \text{ (ring shaped electron beam)} \tag{2.12}$$

if the electron beam spreads uniformly along the radius r_b,

$$G = 1 + ln\frac{r_0}{r_b} \text{ (electron beam in uniformly distributed structure)} \tag{2.13}$$

In the case of $I_b > I_{SCL}$, electrons oscillate at a distance as far as the anode – cathode gap just behind the anode. Potential fluctuations in the virtual cathode create fluctuations with current density oscillating below the virtual cathode and returning to the anode. This situation will be seen in the simulation results clearly.

Virtual cathode oscillations happen approximately at relativistic plasma frequency (f_p).

$$f_p = \frac{1}{2\pi}\left(\frac{n_b e^2}{\varepsilon_0 m\gamma_0}\right)^{1/2} = 8.98x10^3\left[\frac{n_b(cm^{-3})}{\gamma_0}\right]^{1/2} Hz \tag{2.14}$$

here:

- n_b, electron density passing through the anode
- -e and m; electron charge and mass respectively
- ε_0, permittivity of a free space

By substituting the units the following equation is obtained:

$$f_p(GHz) = 4.10\left[\frac{J(kA/cm^2)}{\beta\gamma_0}\right]^{1/2} \quad (2.15)$$

Here $\beta = \frac{v_b}{c} = (1 - 1/{\gamma_0}^2)^{1/2}$ and $v_b$are the electron velocities.

Virtual cathode frequency (f_{VC});

At the nonrelativistic boundary; $\gamma_0 \cong 1$, $\beta \propto V_0^{1/2}$ ve $J \propto V_0^{\frac{3}{2}}/D^2$ Therefore:

$$f_{VC} \propto \frac{V_0^{\frac{1}{2}}}{D}(nonrelativistic\ )$$

Under relativistic conditions, $\gamma_0 \cong V_0$, $\beta \cong 1$ ve $J \propto V_0^2/D^2$ Therefore:

$$f_{VC} \propto \frac{1}{D}(relativistic) \quad (2.16)$$

In relativistic conditions, higher voltage levels are required for HPM systems. However, the voltage dependence of the vircator frequency decreases at voltage values above 500kV. In addition to the oscillation of virtual cathode, the electrons reflecting from real to virtual cathode oscillate in the same region and they also contribute to the microwave emission. Reflexing microwave frequency emitted from here:

$$f_r = \frac{1}{4T} = \frac{1}{\left(4\int_0^d dz/V_z\right)} \quad (2.17)$$

- D represents the distance between anode and cathode,
- V_z is the axial velocity of electrons between the virtual and real cathode for nonrelativistic case,
- T is the time elapsed for the electrons travelling in between the real cathode and virtual cathode

In this case;

$$f_r(GHz) = 2.5\frac{\beta}{D(cm)} \tag{2.18}$$

3. COMPONENTS OF THE VIRCATOR

In order to drive the HPM devices, such connection devices are used as a pulse forming network or a power feedthrough, and high voltage is transferred into the vacuum tube. Electric field simulations can be done to optimize the feedthrough requirements.

HPM generator is fed by a Marx generator. Marx generator is controlled by a fast charging unit. If it is desired to have a repetitive Marx generator operation, charging inductance is used to decrease the RC time constant value. Otherwise, repetition rate of the charging system will be limited. The schematic diagram of the vircator system is:

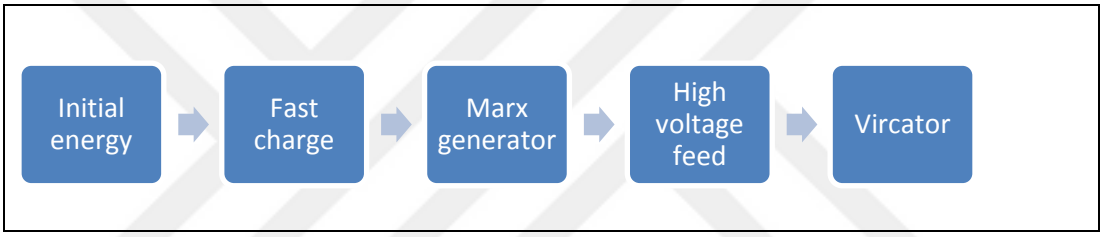

Figure 3.1: Vircator system.

3.1. Marx Generator

In Marx generator, first capacitors which are connected in parallel are charged. Then, high power and high voltage electrical pulse is attained by discharging the capacitors which are set in series connection by switching. After the charging voltage is applied, each capacitor in all stages will have the same voltage using the charging resistors. Total voltage value of the Marx generator is charging voltage times number of stages n.

The Marx generator which is used in this study has 20 stages. It has an open-circuit peak voltage of 400kV, and a matched-load peak voltage of 200kV. Voltage value of the generator can be adjusted by changing the charging voltage value and the pressure of the compressed dry air at the spark gaps. The pressure of the compressed dry air gas affects the discharge voltage of the spark gaps.

Total pulse length of the Marx generator is around 500-600 ns. High power electrical pulse which is the output of the Marx generator is transferred into the vacuum tube by a proper power feedthrough. Applied pulse length is appropriate to remove electrons from the cathode of the vircator.

Recovery time is a fundamental parameter for a repetitive Marx generator. High purity compressed dry air which has a fast recovery time provides generating pulses with high repetition rates. Heating is a problem for repetitive systems. It can be solved by using compressed nitrogen in the vicinity of spark gaps for cooling.

3.2. High Voltage Feedthrough

High voltage feedthrough is used to transfer the pulse which is generated by the Marx generator avoiding deterioration of its shape and structure. For this purpose, a proper feedthrough is used which is shown in the figure below.

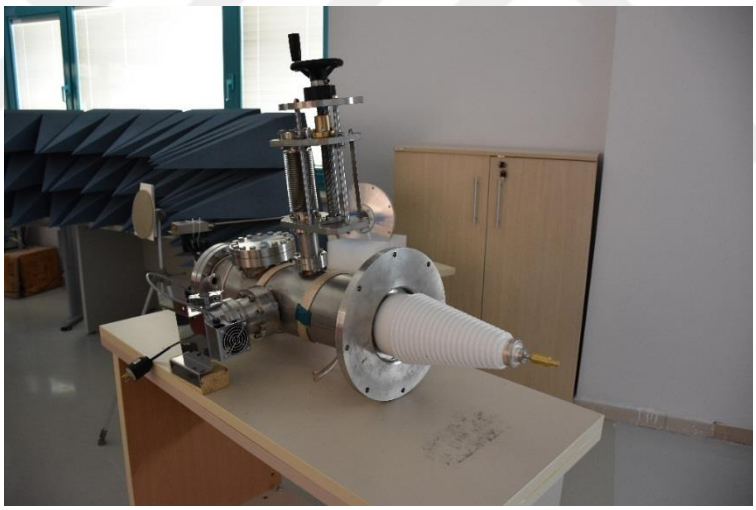

Figure 3.2: High voltage vacuum feedthrough.

The white conical part of the feedthrough can be made of ceramic or Delrin which is a synthetic polymer. The feedthrough which is used in this study is made of ceramic. Central conductor of the feedthrough can be made of brass or aluminum. A feedthrough is a crucial element of a vircator system. It must not change the shape of the initial signal. Thus, it must be a vacuum leak proof feedthrough. Impedance

matching condition of the feedthrough must be considered, and it should be made with high precision.

3.3. Vircator Cathode

Main vircator cathode materials can be grouped as metal, graphite, metal ceramic, carbon fiber and different types of velvet. Cathodes which have long life, low work function, uniform emission and high current density are preferred.

Electrons are emitted into the diode region by explosive electron emission. Explosive electron emission occurs when the electric field on the surface of the cathode exceeds the surface potential barrier limit which is required for electron emission. As electric field value increases, emission current density also increases. It leads to the evaporation of the micro protrusions, and the plasma is observed. The plasma (organic components of the velvet or the evaporated metal) is in the diode region of the vacuum tube. Positive ions move towards the cathode while electrons are accelerated towards the anode and form electron beam.

A fine cathode is obtained providing a homogeneous plasma environment. Furthermore, reproducibility and ease of production of the cathode are also important.

In the literature, there are six types of cathodes. There are some examples below. Similar techniques were used for these cathodes for different dimensions. Several studies claim the most efficient cathode type is velvet coated aluminum.

Figure 3.3: Cathode types: a) Velvet, b) Carbon fiber, c) Chemically etched aluminum, d) CNC machined aluminum, e) Chemically etched copper, f) Pin array cathode.

For high power microwave devices, narrowing of the anode-cathode gap because of the plasma and impedance decreasing are major problems when working with high voltage (>100kV) and current (>1kA). It is supposed that outgassing occurs mainly at the cathode, but it is also occurred at the anode. The velocities of the gas and plasma are around 1 – 10 cm/μs, and this leads to a narrowing of the anode-cathode gap of a few millimeters.

Recently, the most frequently used cathode materials are the carbon based materials. It is found that pure metal or metal based cathode materials which are used in the past degrades in time and have significant amount of outgassing levels. Therefore, velvet and carbon fiber cathode materials are used which have advantages such as efficiency and ease of use.

Carbon fiber, carbon velvet, and graphite are the most widely used cathode materials for pulse mode high power microwave generators. Carbon fiber is one the most suitable cathode materials to achieve high current with the properties of high electron beam emission, nanoseconds starting time, convenience of usage in the

vacuum environment, and long life time. These types of cathodes are made by pyrolytic connection of carbon fibers to carbon surface or to metal surface with conducting epoxy. In this study, there are used three different cathode types. First, steel cathode was directly used. Second, graphite was bonded to steel surface using epoxy with silver additive. However, the most stable and proper microwave signals were extracted using a cathode which has velvet bonded to steel surface using conductive epoxy. In cathode production, there are three essential criteria:

- Materials which have low outgassing levels should be chosen as emitting materials.

- Production stages should be controllable and repeatable.

- Cathodes with long life should be chosen, and they must endure to repetitive pulsed operation.

3.3.1. Velvet Cathode

Velvet is coated onto the steel surface using electrically conductive epoxy as shown below.

Figure 3.4: Velvet cathode model.

This material is both cheap and easy to process, but it has some disadvantages such as durability.

Velvet has low electric field threshold level to form plasma, proper emission, and low anode-cathode gap narrowing rate. However, it is not suitable for repetitive operation because significant amount of the material is lost during the applied pulse. Its life time is also limited because of the erosion of the tufts.

Velvet cathode is composed of tufts on the surface. Each of them consists of approximately 40 fibers which are 10-20 μm in diameter. In the figures below, there are scanning electron microscope (SEM) images of the velvet.

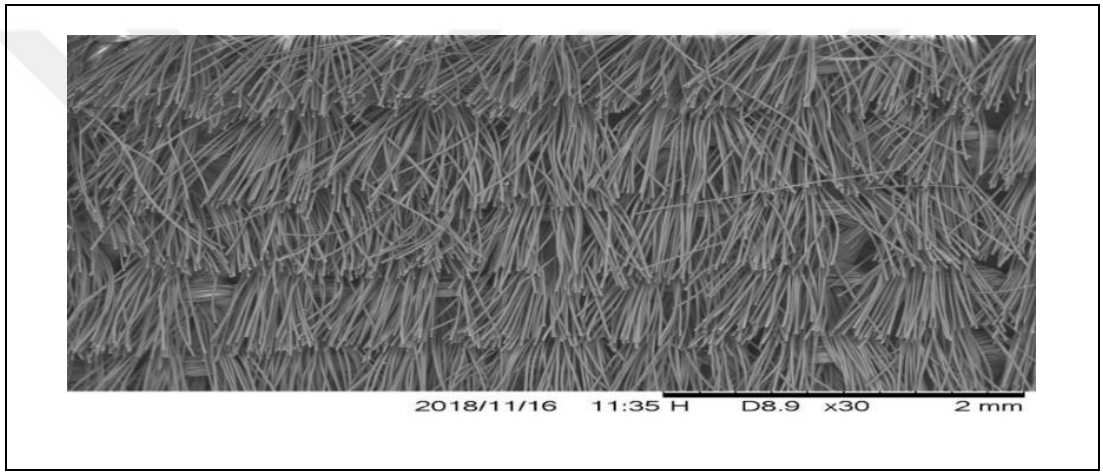

Figure 3.5: SEM image of the velvet.

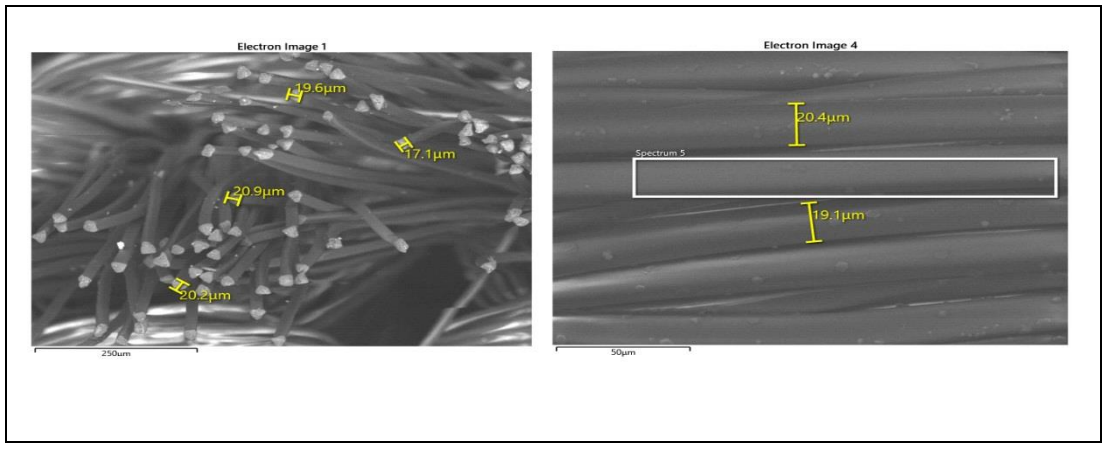

Figure 3.6: Tuft structure of the velvet.

To sum up the studies of the velvet cathodes which work by explosive electron emission mechanism:

When the electric field value exceeds 16 kV/cm, plasma occurs on the surface. The characteristic polarization formation time of the velvet tufts is around 90 ns. If the rise time of the voltage signal exceeds a few 10 nanoseconds, in order to calculate the voltage value of the time when the flare is appeared, tuft polarization process should be considered.

Surface flare causes the loss of velvet material and outgassing from the surface. Amount of the material released from the standard velvet material which has linear density (12 tufts/cm) is approximately $3x10^{15}$mol/cm^2. Average density of the vapor in the volume of tuft region is 10^{18}mol/cm^3, and it is at the room temperature. The erosion rate limits the maximum life time of the velvet cathode.

If the velvet cathode is used in the repetitive mode, material which are released from the cathode surface causes a pressure increase in the environment. This limits the repetition rate. The source of this limiting process is considered as the avalanche breakdown between the anode and the cathode. Pressure is inversely proportional with the pulse time at the time of the anode-cathode narrowing or when plasma starts to close the gap.

Gas columns which are produced by surface flare consist a significant amount of electrons. Applied electric field leads to the electron current from the ionized gas columns which are restricted by the space charge limit. Current which occurs along the tufts heats the vapor. Thus, temperature determines plasma closure rate between the anode and the cathode. The lower limit of the plasma closure speed which is obtained by this approach is given by the formula below.

$$V(m/s) = 100(d^*/D)^{3/2}V^{1/2} \quad (3.1)$$

In the equation, d* is the distance between velvet tufts, D is the anode-cathode gap, and V is the applied diode voltage. The increase in the diode perveance which arises from the plasma formation brings an upper limit for pulse length. When working with moderate repetition rates, it is observed that flare threshold value increases, closure rate of the anode-cathode gap increases, and the repetition rate

itself increases a little bit. When the cathode is used frequently, it preserves the initial working conditions.

One of the most important features of the velvet cathodes is proper emission because tufts contribute the emission equally. The tuft length and the distance between the tufts are comparable physical dimensions. Short tuft length and closeness to the metal surface disrupt equipotential curves of the flare which occurs along a single tuft.

3.3.2. Polymer Velvet Cathode

One of the most successful cathode materials which are used in the HPM studies is polymer velvet. It has low electric field threshold value, proper emission, and low plasma closure rate between the anode and the cathode. Expansion of the plasma in the anode-cathode gap decreases the diode impedance. It shortens the high voltage pulse.

The electron current density value is $<100 A/cm^2$ in the electron beam emission experiments in the literature. For an intense electron emission, cathode materials which are used in the past are also tried on carbon fiber and carbon velvet. It is determined that carbon fiber structure has a longer life time than polymer velvet. Additionally, these can be coated with CsI salt. Velvet cathode can resist higher currents ($7 kA/cm^2$), but this is valid for short pulse lengths.

Velvet cathode is also used in the magnetically insulated line oscillators (MILO) which generates high power electromagnetic signals, do not need external magnetic field, and generates short pulses. In this way, damages in the vicinity of the cathode are minimized, and the life time of the cathode is increased. Additionally, electron production in each shot results better. One of the most crucial topics about the HPM devices is statistical variation of the microwave signal. Maximum power value and the pulse length of the microwave signal can change after each shot. This can be caused by the change of effective cathode emission area and instability of the plasma closure rate.

Polymer velvet cathode has a lower threshold energy value than graphite cathode. Time dependent impedance and perveance values can be calculated using the voltage and current waveforms.

When the cathode materials graphite, stainless steel, and red polymer velvet are compared; velvet provides high current density with its superior emission characteristic. It has also the lowest plasma expansion rate among these materials. It also shows the smaller variation between the shots and voltage delay is also the lowest among these cathode types. However, at high current density levels, material degrades and the emission of the cathode decreases.

3.3.3 Carbon Fiber and Velvet Cathode

Carbon fiber cathodes have longer life than velvet cathodes, and they can be coated with CsI salt. Thus, emission threshold level decreases, electron beam emission uniformity and cathode life increases. Carbon fiber cathode is different when compared to the standard velvet cathode with tufts. Although their surface morphologies are similar, hydrocarbons are not used during the production of carbon fiber cathode.

Cathode samples can be prepared by two ways. First, carbon can be bonded on the metal surface using epoxy. The epoxy is a partially volatile substance and it is preferred because it has low outgassing rates.

Secondly, carbon fibers can be attached on carbon surface. In this configuration, there is no volatile substance. Then, it has not a negative effect for the vacuum environment. Thus, since it has lower outgassing levels, its performance is higher.

Diameter and height of the fibers are 10 μm and 1.5 mm, respectively. Previous studies show that polymer velvet cathode shows outgassing of 10 atoms or higher; whereas, CsI coated carbon shows 5.8 atoms of outgassing.

Table 3.1: Comparison of the coated and the uncoated cathodes

Cathode type	**Outgassing (atom / electron)**	**Difference with coated carbon fiber (%)**
Uncoated – carbon on epoxy (CE)	4.7	10.1
Uncoated – carbon on carbon (CC)	4.0	18.4
Coated – carbon on epoxy (CE)	4.0	18.4
Coated – carbon on carbon (CC)	3.5	24.7

In summary;

- Carbon fiber cathode is more advantageous than polymer velvet cathode.
- Polymer velvet cathodes are unfavorable in terms of life time.
- CsI coating decreases the impedance decline, lowers the electric field threshold level and lowers the outgassing rates.

In the figure below, carbon fiber which is produced by ESLI [1] company is bonded on aluminum surface using epoxy. In this structure, height and diameter of the fibers are 1 mm, 7 μm, respectively.

Figure 3.7: Carbon fiber cathode.

3.3.3. Chemically Etched Aluminum and Copper Cathode

In a study which is done by Yeong-Jer Chen [1], [2] in Texas Tech University, a cathode is prepared by aluminum etching technique. The standard wet etching technique is used in the preparation of the cathode.

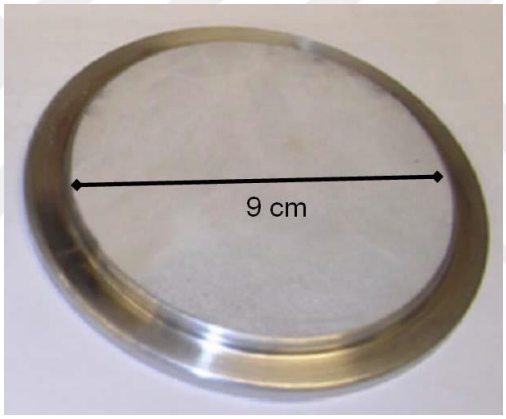

Figure 3.8: Etched aluminum cathode.

9 cm diameter, 6061 aluminum disk is used in this cathode type. The widths of the canals are 40 μm and the heights of them are 150 μm. The canals are made by the standard aluminum etching technique. The acid solution is composed of phosphoric acid, water, nitric acid, and asetic acid (16:10:1:1:H3PO4:H2O:HNO3:CH3COOH). This solution is applied a certain time on aluminum disk which is prepared by photoresist technique. Then, the desired dimensions of the canals can be obtained. Figure 3.9 shows the optical interferometer images of the canals which have depths of 100 μm and 150 μm. The application time of the chemical acids is very important

during the etching process. For this reason, determining the optimum duration of the application of the chemical acids is crucial. If the optimum duration is not achieved, the etching may occur more than requested, and deterioration may occur as shown in Figure 3.9.

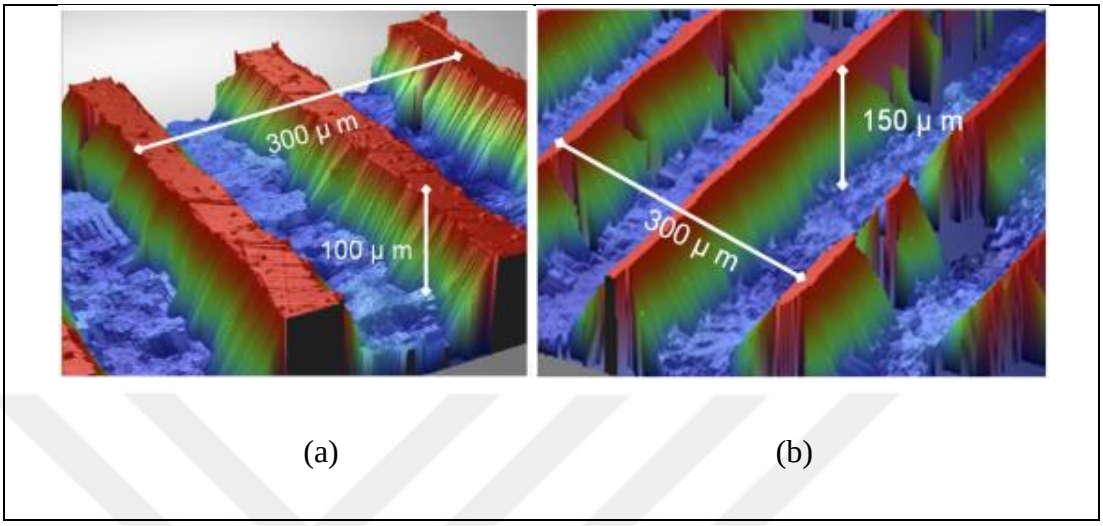

Figure 3.9: Optical interferometer images of the canals on the aluminum cathode a)100 µm canals b)150 µm canals.

Last, when the etching process is completed, edges of the cathode can be excavated and the surface can be polished. Figure 3.8 shows the finished aluminum cathode which is 9 cm in diameter and has the homogeneous canals of 100 µm depth [1].

3.3.4. Pin array Cathode

In this cathode type, carbon fibers are placed on stainless steel surface as in the studies in the literature. Carbon fibers should be upright position and remain together, so they are bonded on the surface with conductive epoxy. This cathode type was produced and used in the vircator system. Nevertheless, the results are poor when compared to results which are obtained using velvet and graphite cathodes.

Figure 3.10: Pin array cathode structure.

3.3.5. Graphite Cathode

Different cathode types are experienced for explosive electron emission. These are velvet, carbon fiber and high degree graphite. Velvet cathode has low electric field threshold value, high outgassing rates, and a limited life time. Carbon fiber cathode has also low electric field threshold value, low response time to pulse, and low plasma expansion rate. Graphite cathode is low cost, has long life, low outgassing rates, and is the most stable one for repetitive operation. On the other hand, graphite has lower current density than the other cathode types.

Figure 3.11: Graphite cathode

Micro protrusions which are a few micrometers exist on the cathode surface. Local electric field value may be 10000 times higher at these points. Thus, an intense electron emission occurs. These points are the initial emission points, so abrupt temperature increase occurs at these points. Because of the temperature, at the tips of the micro protrusions plasma is formed which appears as explosion. The electrons emitted from the plasma reaches to the anode-cathode gap, and diode impedance decreases. When the formed plasma at some regions behave as a shield for other regions, and the electron emission does not occur. For this reason, a time delay occurs between the instant when the voltage is applied and the instant when the current is obtained. Delay time depends on the work function of the cathode and the shape factor.

Graphite with narrow granular structure provides a better electric field formation. If the distance between the initial emission regions becomes smaller, the propagation time of the plasma through the surface decreases. Then, delay time also decreases.

When the grain size becomes larger, electron emission uniformity starts to deteriorate for the graphite cathodes. Thus, emission regions will be fewer in number

and formed plasma shields other emission regions. Consequently, the current density and the life time decrease.

3.4. Anode Structures of the Vircators

Anode material of a vircator is crucial since this component is responsible for the impedance decrease. This leads to the plasma formation which causes the anode-cathode gap narrowing. The temperature at the surface of the plain metal anodes causes outgassing. The polishing process which is applied on the anode surface reduces the outgassing a little bit, but it is still at the undesired levels.

A decent vacuum level is required for the moving electrons in the vacuum tube. 10^{-4} and 10^{-6} torr pressure levels are enough for high power microwave generation.

Both the anode and the cathode materials are crucial for the generation of the microwave signal. Experiments show that usage of a molybdenum anode material provides more stable microwave generation when compared to other anode materials. The anode structure can be a grid or a thin film. The thin film transparent foil must have a thickness much smaller than the mean free path of the electrons. For the nonrelativistic case the anode can be made as web. In this study, voltage values are not high like 400 kV, so stainless steel with honeycomb form is preferred for the anode. Studies show that the transparency of the anode should be 50-70% for high power microwave applications [19], [20]. Virtual cathode oscillation region must be high enough if a high value of anode transparency is chosen. Experiments show that the transparency of the anode is linearly proportional with the microwave output power. However, for the repetitive operation, higher anode transparency deteriorates the microwave signal generation.

Figure 3.12: Photograph of the stainless steel anode mesh

Honeycomb structure is the most suitable for the anode when the studies which examine the anode transparency in the literature are investigated. Using this structure higher transparency can be obtained specially for the circular anode. In the vircator of this study, a 70% transparent anode is used which has a thickness of 0.80 mm. Dimensions of the holes are 3.25 mm and the distance between the holes are 3.70 mm. Figure 3.13 shows a design which is done by CST, and it is used in the simulations.

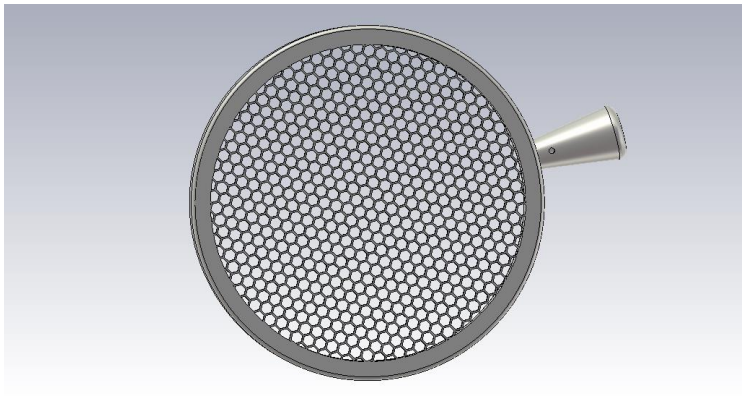

Figure 3.13: Aluminum anode structure.

3.5. Types of Vircator

Vircators can be designed in several different types. The most common of these are; Axial, Coaxial and Reflex triode vircators. The axial and reflex triode are also parallel to the anode-cathode, while the coaxial vircator also the anode and cathode cylinder have the same central axis. In addition, a positive pulse is applied to the reflex triode vircator anode. In axial and co-axial vircators, negative pulses are generally applied to the cathode.

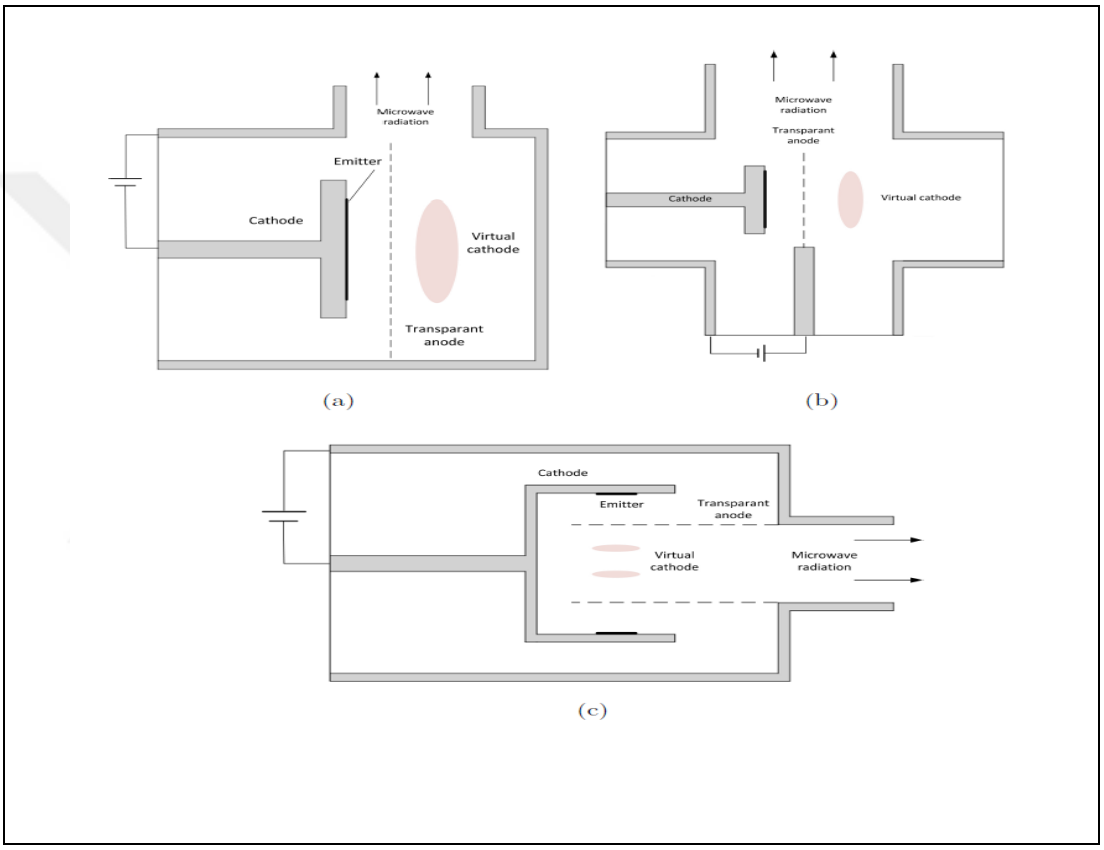

Figure 3.14: 1) Axial Vircator, 2) Reflex Triode Vircator, 3) Coaxial Vircator.

In contrast to this, Reditron is more frequently reported in the literature [3]. Unlike the above examples, the anode is designed to be slightly thicker in order to prevent the reflected electrons from passing back into the diode region if only the magnetic field is applied. It is divided by narrow slits between anode structures.

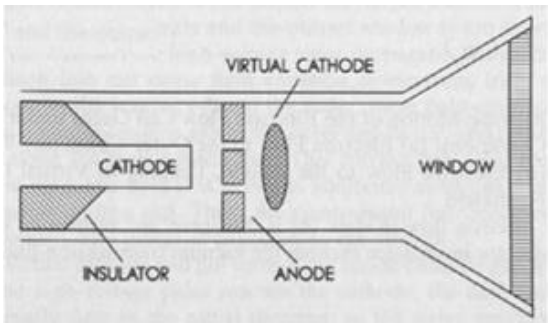

Figure 3.15: Reditron.

In order to improve the performance of the vircator structures, the virtual cathode must be located in a space called resonance cavity. It is possible to obtain higher areas when this cavity can be adjusted to the operating frequency. Axial and Reflex triode are also designed as hollow box in this field. The space between the cathode and the anode in the coaxial vircator naturally forms this area.

3.5.1. Axial Vircator

The structure is the simplest model of the vircator. However, since the distance between the anode and cathode is constant, it does not allow any changes during the study, thus slowing the studies in this thesis. In addition, the cavity around the virtual cathode can be precisely determined. In this way, it is easier to produce a vircator at the desired frequency. Only the distance between the applied voltage and the anode cathode is important for the efficiency of the microwave produced.

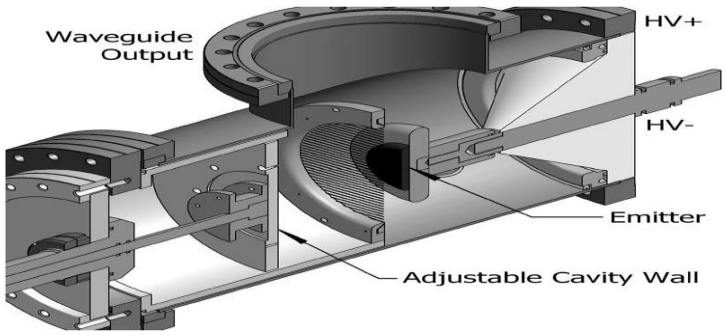

Figure 3.16: Axial Vircator Structure.

3.5.2. Reflex Triode Vircator

The main advantage of the reflex triode vircator is that the distance between the anode cathode is easily adjustable. The disadvantage is that the cavity around the virtual cathode is not fully formed in the configuration examined in this thesis. This causes unstable frequency generation. Again, in the reflex triode vircator, the current path is not straight. The magnetic field around the changing electric field generates a Lorentz force caused by deviations in the electron beam. In other words, this creates energy loss. If the resonance cavity is used, this loss can be minimized. Simulation studies have shown that the reflex model can work much more efficiently than the axial model.

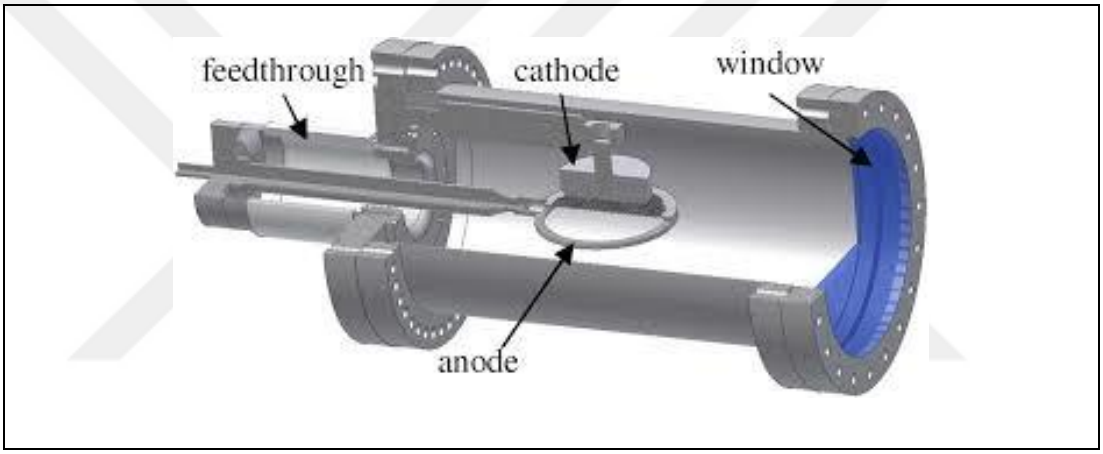

Figure 3.17: Reflex Vircator Structure.

3.5.3. Coaxial Vircator

The emitter position is arranged cylindrically on the anode in the coaxial vircator. This type of design is intended to move freely. The cathode cylinder can also move axially when the distance between the cathode and the anode changes. The cathode cylinder is formed by attaching the emitter material to the metal cylinder structure by means of an adhesive.

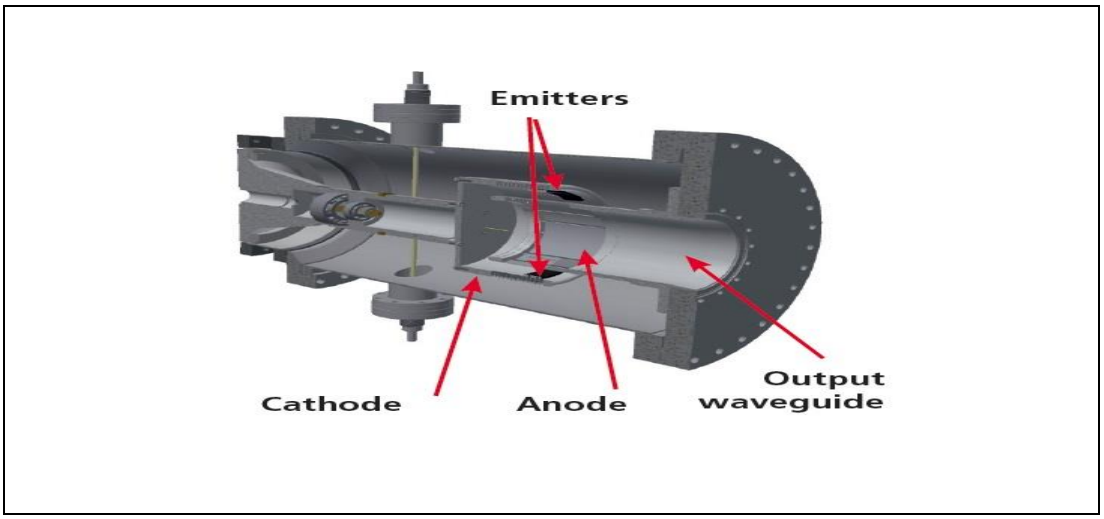

Figure 3.18: Coaxial Vircator Structure.

The electron beams formed by the areas in which two opposing emitter materials are bonded mutually repel each other and form the virtual cathode at a certain distance in the middle. As a result of these pushes, when the virtual cathode vibrates and reaches a certain frequency value, a high power microwave is produced. When the studies in the literature are examined, the highest yield is obtained in this structure but there is not yet a commercially produced model as far as we know.

3.5.4. Multi Cavity Vircator

Although they have the advantages of high power capability in microwave production and the ability to adjust the operating frequencies, they have remained secondary for a long time due to their low efficiency compared to other generators. However, with the understanding that the efficiency of the vircator is highly dependent on the intensity of the electromagnetic field around the virtual cathode, in order to obtain more efficient electromagnetic field, the researcher intensified research on improving the structure in the form of modulation of virtual cathode. [48] Recently, different types of modified multi-cavity vircators have also been studied to improve power efficiency.

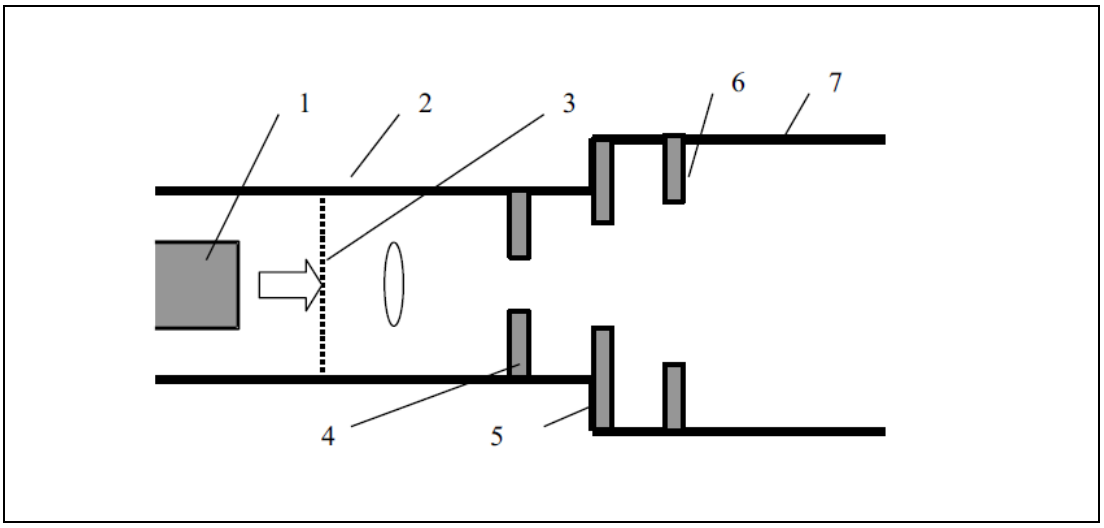

Figure 3.19: Multi Cavity Vircator Structure. 1) Cathode, 2) Waveguide, 3) Anode, 4) First cavity, 5) Second cavity, 6) Third cavity 7) Output waveguide.

4. VIRCATOR SIMULATIONS

Virtual cathode oscillators come into prominence as a microwave source which is thought to be used frequently in the future because of the high power it provides, simplicity of its design and its ability to be adjusted to different frequencies with easy parameter changes. Vircators have wide bandwidth but their efficiency is generally less than 10%.

The particle studio solver (PS) of the CST simulation medium was used for the simulation studies of the vircator systems. PS is a powerful and fast simulation tool especially used for 3D analysis and solution of electromagnetic problems. It is a very good solution especially for the modeling of devices such as electron gun, electron tubes and electromagnetic generators.

4.1. Test of Vircator Cathode Types in CST Simulation Environment

Before the cathode trials, the whole material was selected as the cathode structure. However, electron emission from the corners was observed at a higher rate than the electrons coming out of the cathode surface, this has caused the simulation results to be inaccurate. Therefore, the cathode material was wrapped around the conductive plate by taking the studies carried out in the experimental environment.

Simulations were performed for 4 different cathode materials. These; graphite, aluminum, copper and metal (PEC). The cathode and anode radius were adjusted according to the measurements in the literature examples, and the most suitable anode cathode distance for vacuum tube radius was between 50 - 70 mm and the most suitable intermediate distance was determined as 69 mm. The trigger signal is a rectangular pulse 10 ns rise time and 190 ns operation time, total 200 ns.

4.1.1. Cathode Simulation Results

4.1.1.1. Simulation Studies for PEC Materials

The results obtained from the simulation studies with excellent electrical conductor (PEC), which is a perfect conductor lossless material which CST PS defines as standard, are shown in the following figures.

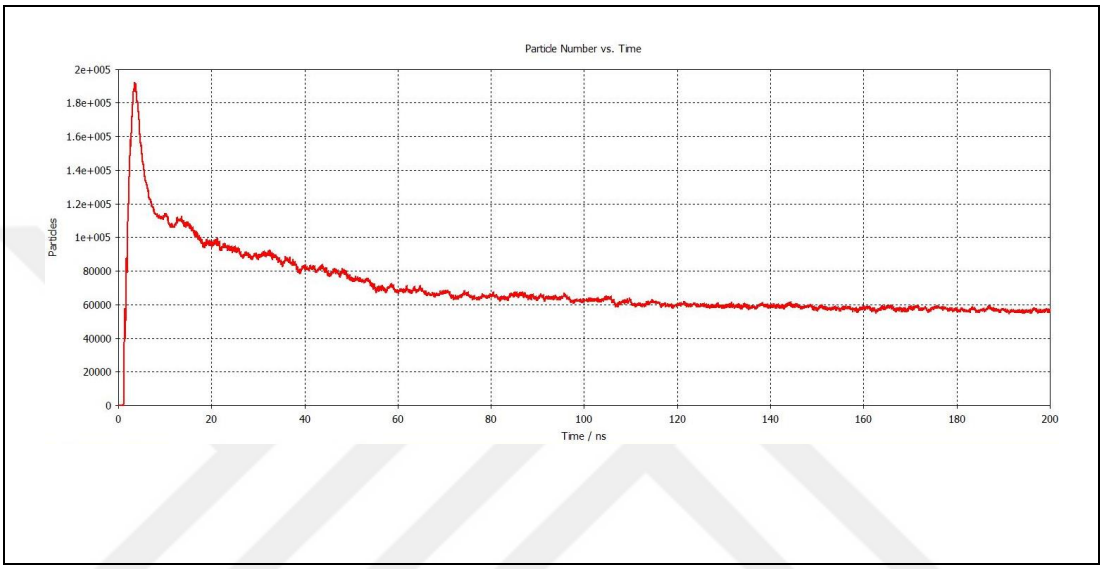

Figure 4.1: Number of Particles - Time Graph (Average Current: 6 kA).

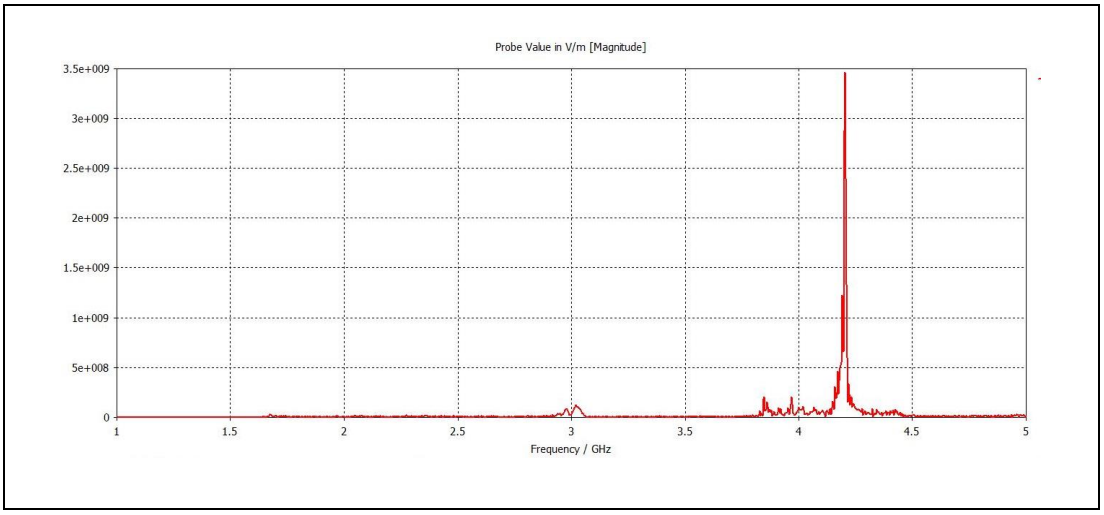

Figure 4.2: Electric Field at 4.2 GHz.

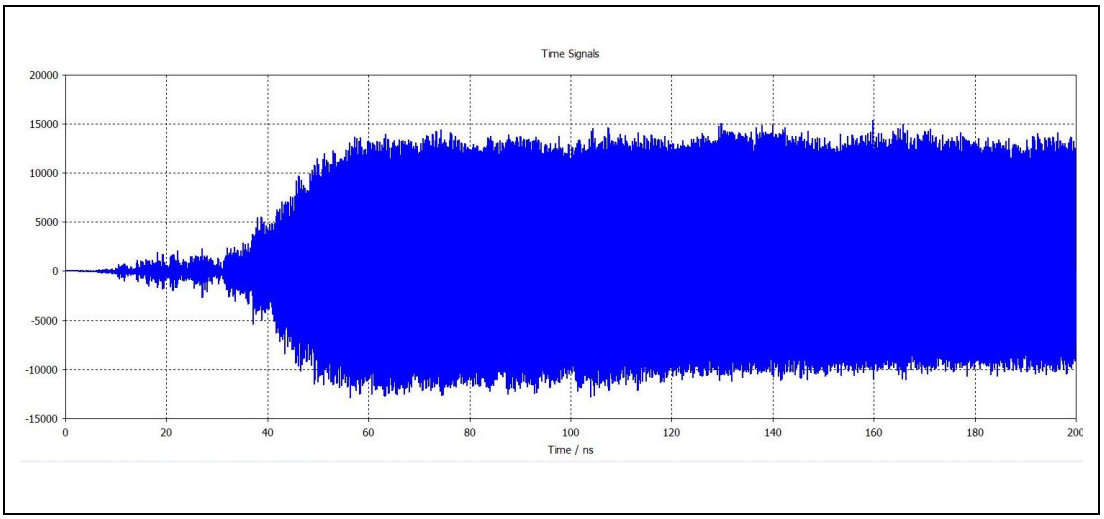

Figure 4.3: Time Dependent Vircator Output Signal.

Maximum efficiency is 11.13%, maximum power is calculated as 235.86MW.

4.1.1.2. Simulation Results for Aluminum Material

The following results were obtained for CST PS simulations using aluminum material for cathode.

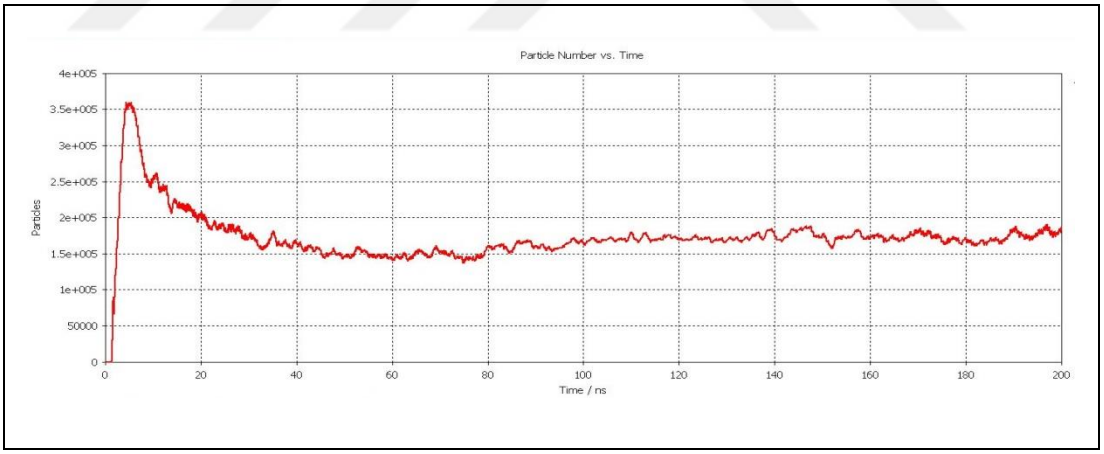

Figure 4.4: Time graph of particle number.

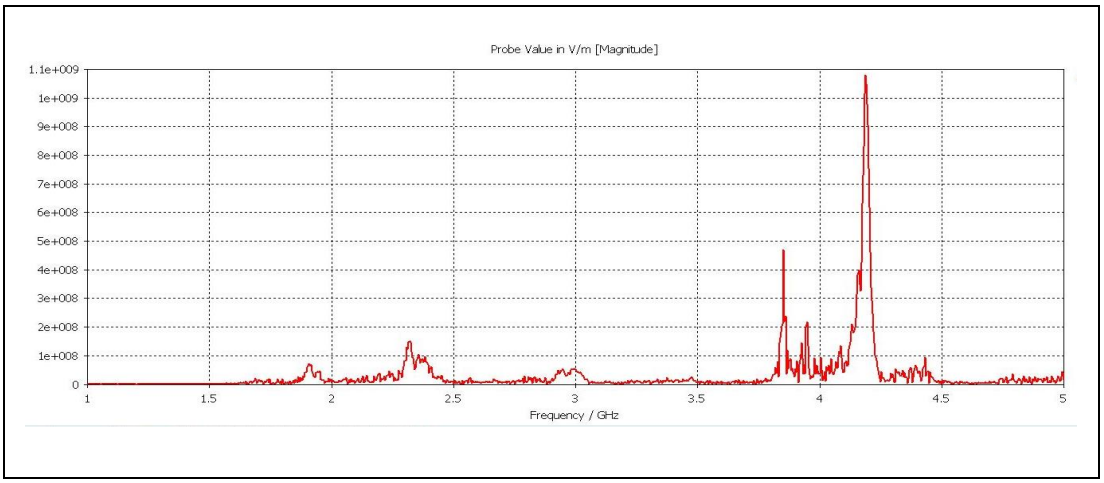

Figure 4.5: Frequency graph of the generated signal.

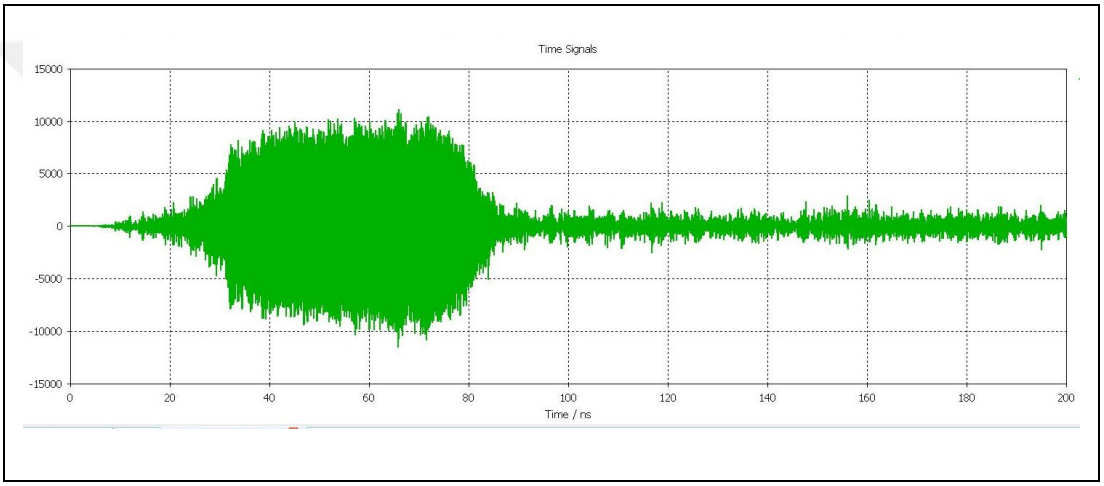

Figure 4.6: Time dependent output signal.

As a result of the simulations, the average current is 5 kA, frequency: 4.2 GHz maximum efficiency: 5.77% and maximum power: 132.55MW.

4.1.1.3. Simulation Results for Graphite Material

The following results were obtained as a result of the CST PS simulation studies using graphite cathode material:

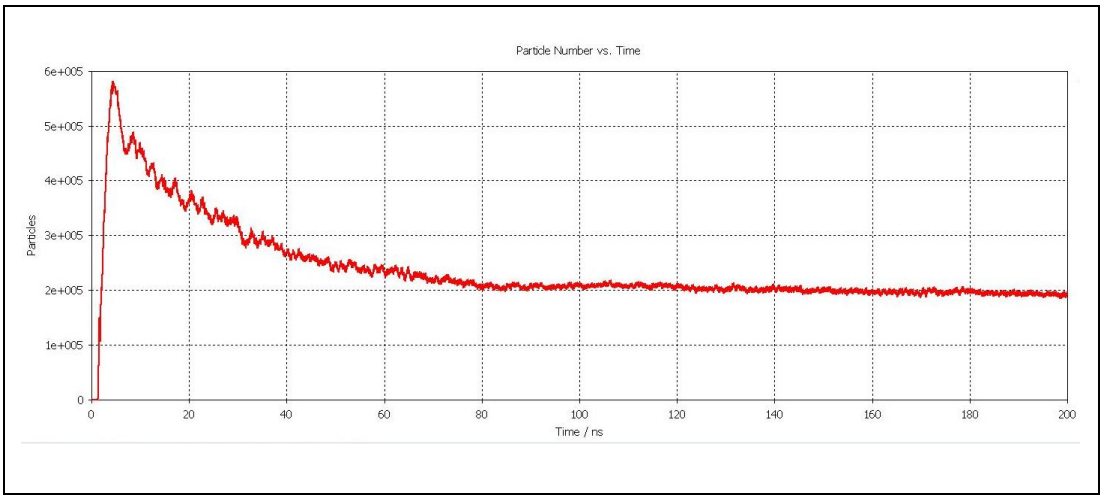

Figure 4.7: Graphite cathode particle graph.

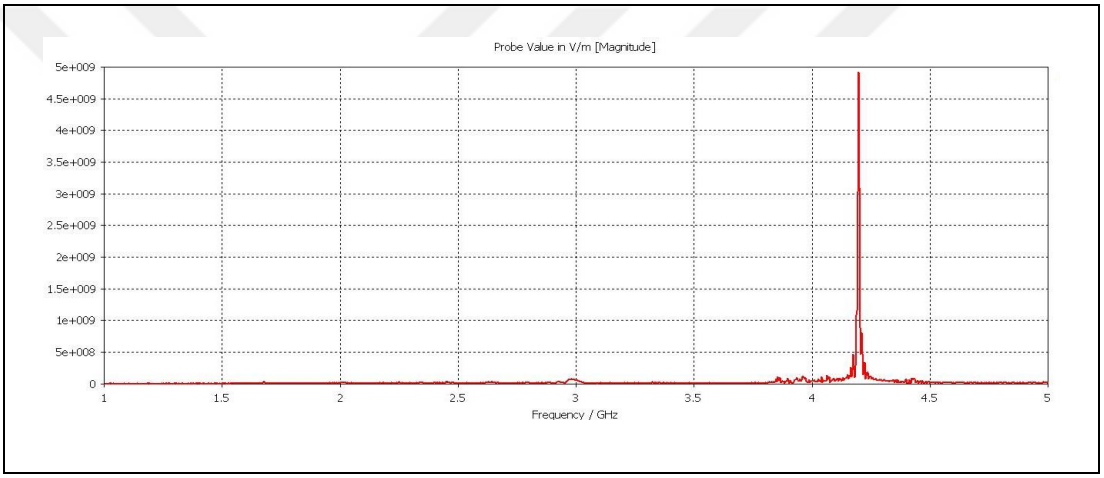

Figure 4.8: Graphite Cathode Frequency Graph.

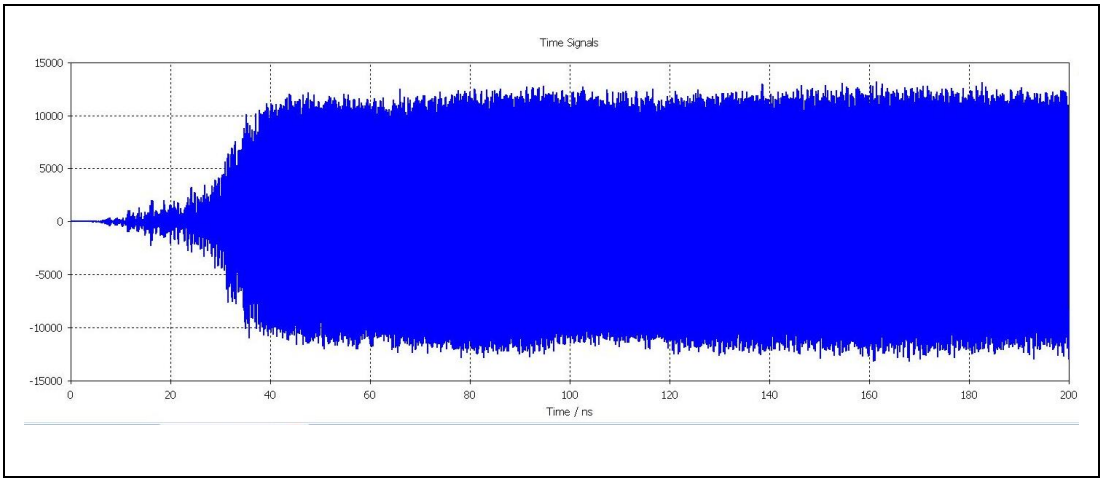

Figure 4.9: Graphite Cathode Output Signal.

When the values obtained from the simulation results are examined, average current is 7 kA, frequency: 4.2 GHz, maximum efficiency: 8.49%, maximum power: 174.02MW.

4.1.1.4. Simulation Results for Copper Material

CST PS simulation results using copper cathode are shown in the following figures:

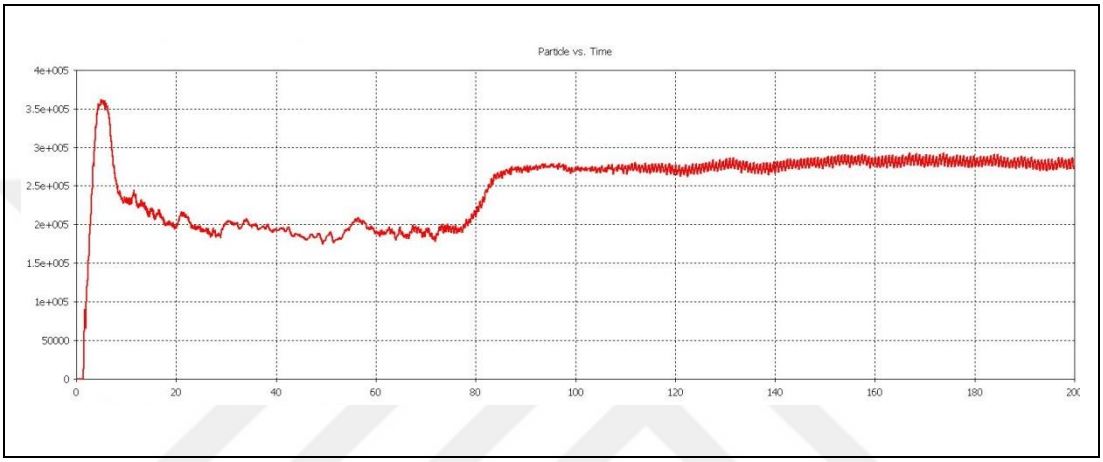

Figure 4.10: Copper Cathode Particle Graph.

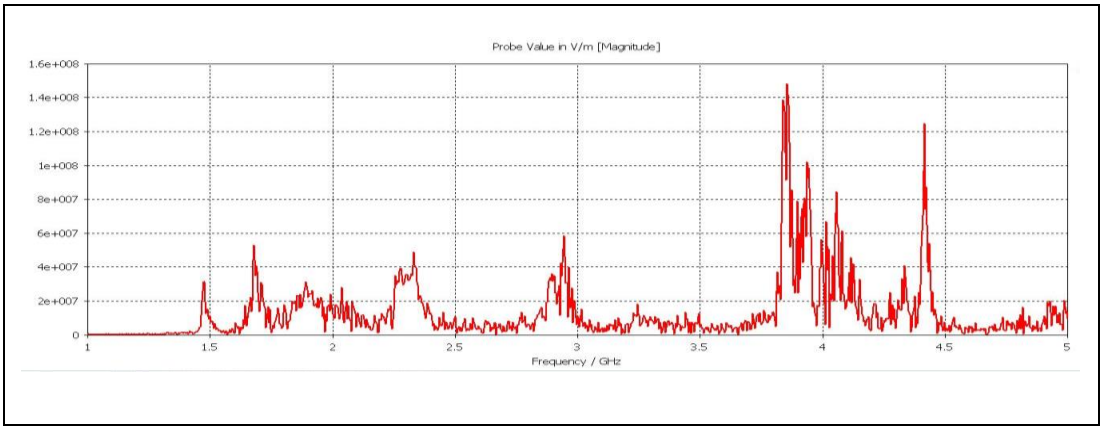

Figure 4.11: Copper cathode frequency graph.

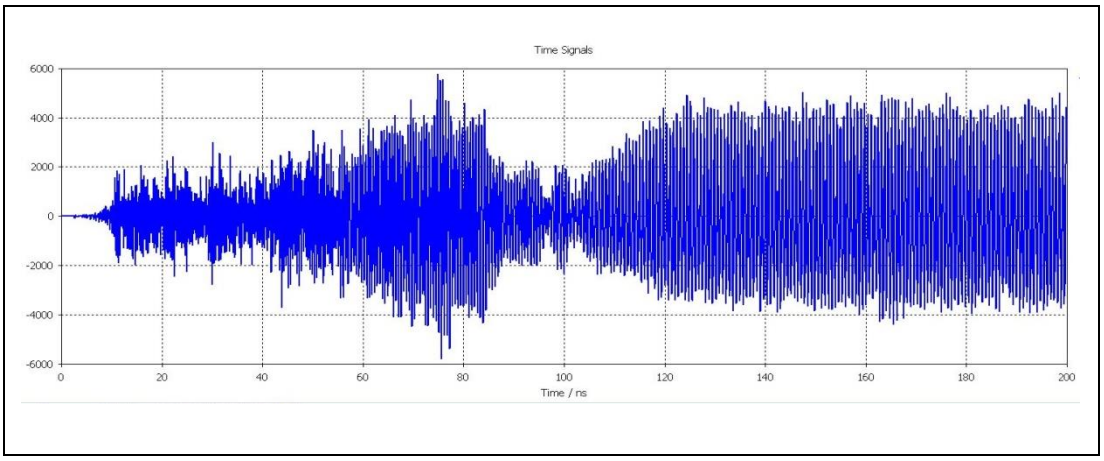

Figure 4.12: Output signal with copper cathode.

When the results of CST PS simulation studies using copper cathode were examined, average current was 1 - 6 kA, frequency 4.2 GHz, maximum efficiency: 2.02%, maximum power was calculated as 33.71 MW.

4.1.2. Evaluation of Results

Table 4.1: Current, efficiency and power values for four different samples.

	PEC	**Copper**	**Graphite**	**Aluminum**
Current (kA)	6	1 - 6	7	5
Efficiency(%)	11.13	2.02	8.49	5.77
Power (MW)	235.86	33.71	174.02	132.55

According to the data in Table 4.1, the highest efficiency and power value is obtained from excellent electrical conductive (PEC) material. However, since this CST software is an ideal material for modeling purposes only and there is no perfectly conductive material between real materials, the choice of graphite material can be considered in practical applications. The most uniform electron radiation and electric field value was obtained with graphite material among real materials.

Graphite and steel materials were used in the cathode structure of the produced vircator.

In addition to these studies, the simulation results were assumed to be experimental data and the values of perveance were calculated. A fit function was found in accordance with these data obtained with MATLAB. Plasma expansion rate and cathode emission initial area values were calculated.

The following equations were used in making these operations. Here, P_{CL} is the definition of the electron flow between two parallel diodes according to the Child-Langmuir Law [49]. R_k is the cathode diameter and vt is the axial velocity of electrons.

$$P_{CL} = \frac{4\varepsilon_0}{9}\left(\sqrt{\left(\frac{2e}{m_e}\right)}\right)\pi\left(\frac{R_k}{D}\right)^2$$

$$R_k = r_0 + vt \qquad (4.1)$$

$$D = d_0 - vt$$

If the constants specified in the equation are replaced with:

$$P_{CL} = 7.33x10^{-6}\left(\frac{r_0 + vt}{d_0 - vt}\right)^2 \qquad (4.2)$$

$$\frac{r_0 + vt}{d_0 - vt} = \sqrt{\frac{P_{CL}x10^6}{7.33}} = y_1 \qquad (4.3)$$

$$d_0y_1 - y_1vt = r_0 + vt \qquad (4.4)$$

$$Y = aX + b \qquad (4.5)$$

$$Y: d_0y_1 \qquad (4.6)$$

$$a: v \tag{4.7}$$

$$X: t(y_1 + 1) \tag{4.8}$$

$$b: r_0 \tag{4.9}$$

The terms Y and X among these expressions are known quantities. P_{CL} expresses the results obtained from the CST. The coefficients a and b are the fit parameters, after which the plasma velocity and the area at the time of cathode emission can be found. MLR (Multiple Linear Regression) method was used for this purpose. The simulations were performed with a positive sinus stimulus signal of 50 ns duration. Signal form is as follows.

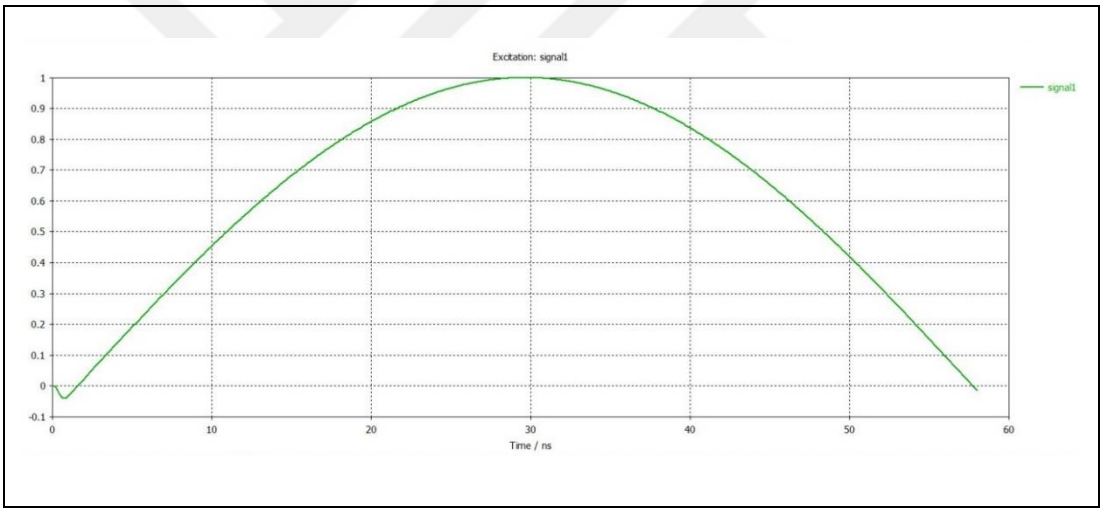

Figure 4.13: Positive Sine Stimulus Signal Form.

The performance data was calculated from $Current/Voltage^{1.5}$. Using this calculation, the formula was written for 4.2 and the equations required for MLR were obtained. Several adjustments were made before these equations were achieved. At the time domain generated in the CST environment, the portion of the microwave signal formed from 10 ns was considered. The data received from this moment on physically has a meaning. The data obtained from this moment were given as input to MATLAB and the values between 0 and 0.0002 were taken into consideration. The

linear equation created by writing this data in Excel was solved. Here v (cm/ns) and r_0(cm) are found as coefficients. The obtained coefficients were replaced with the P_{CL} equation and the theoretical values were obtained. The curves obtained from numerical calculations and theoretical analyzes are shown below for different materials:

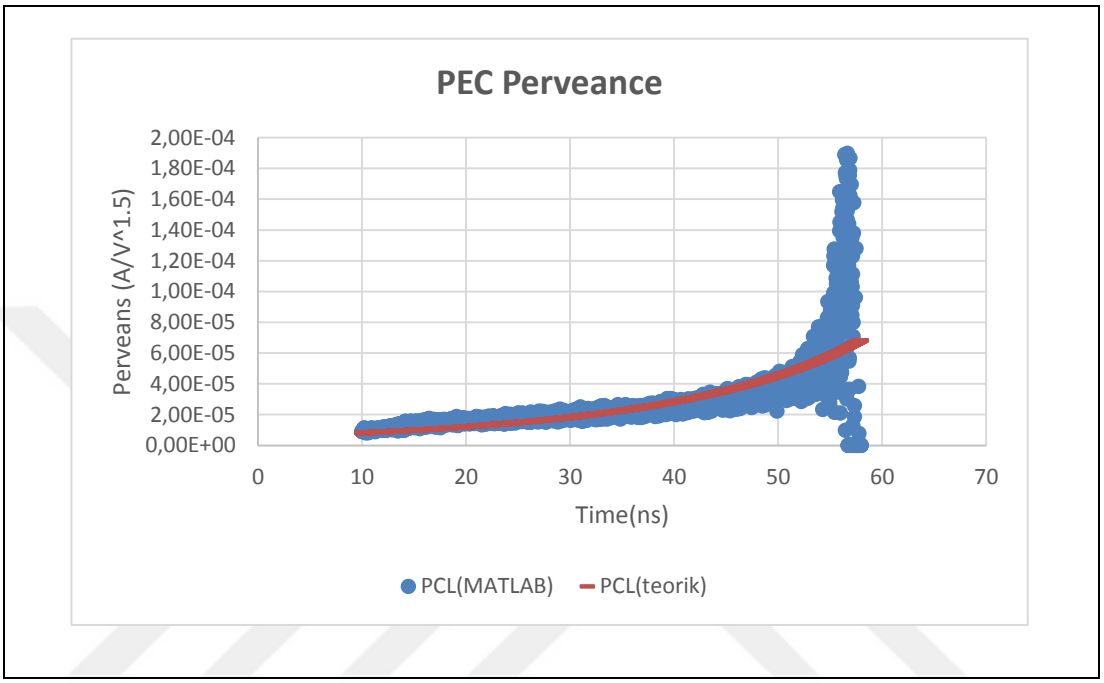

Figure 4.14: PEC Material Perveance.

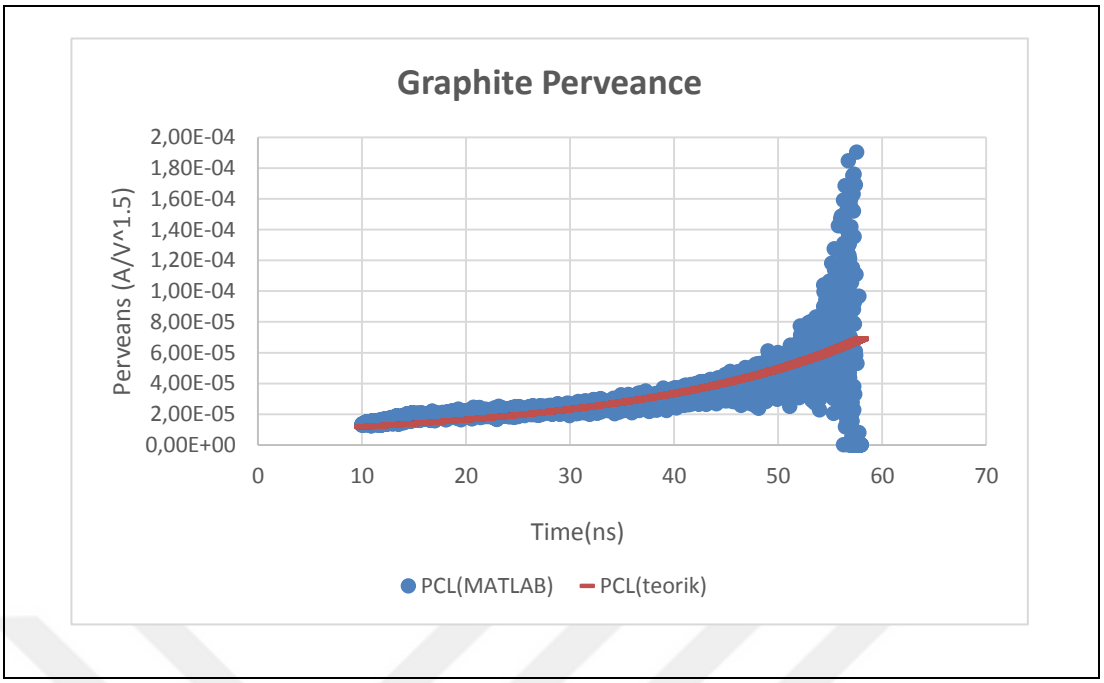

Figure 4.15: Graphite Material Perveance.

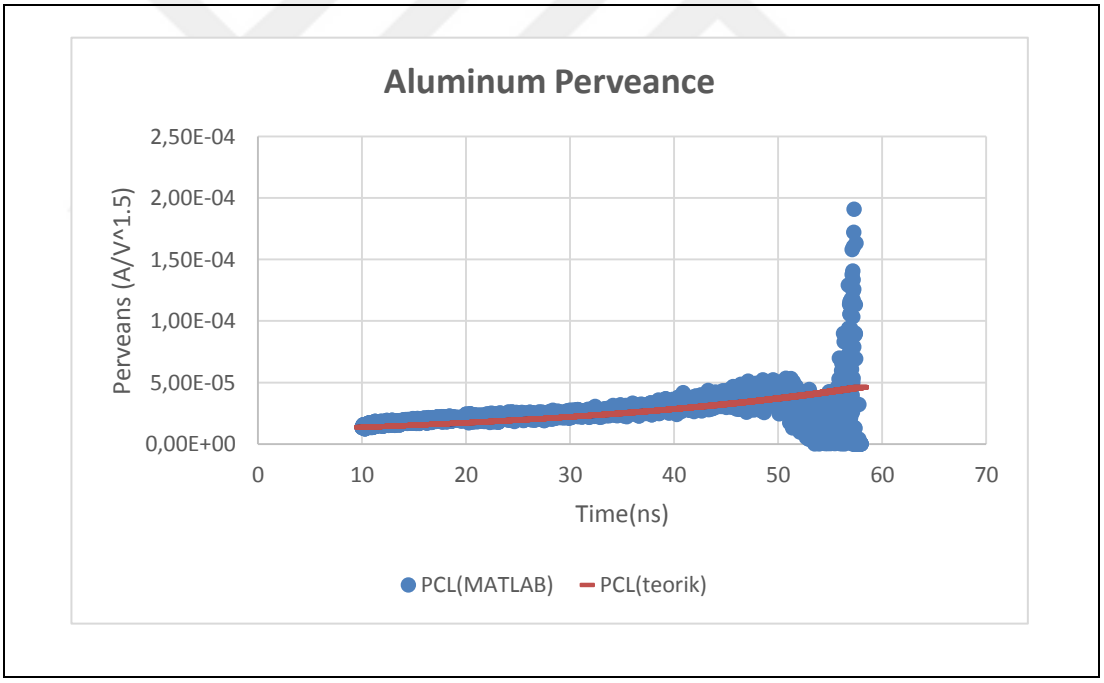

Figure 4.16: Aluminum Material Perveance.

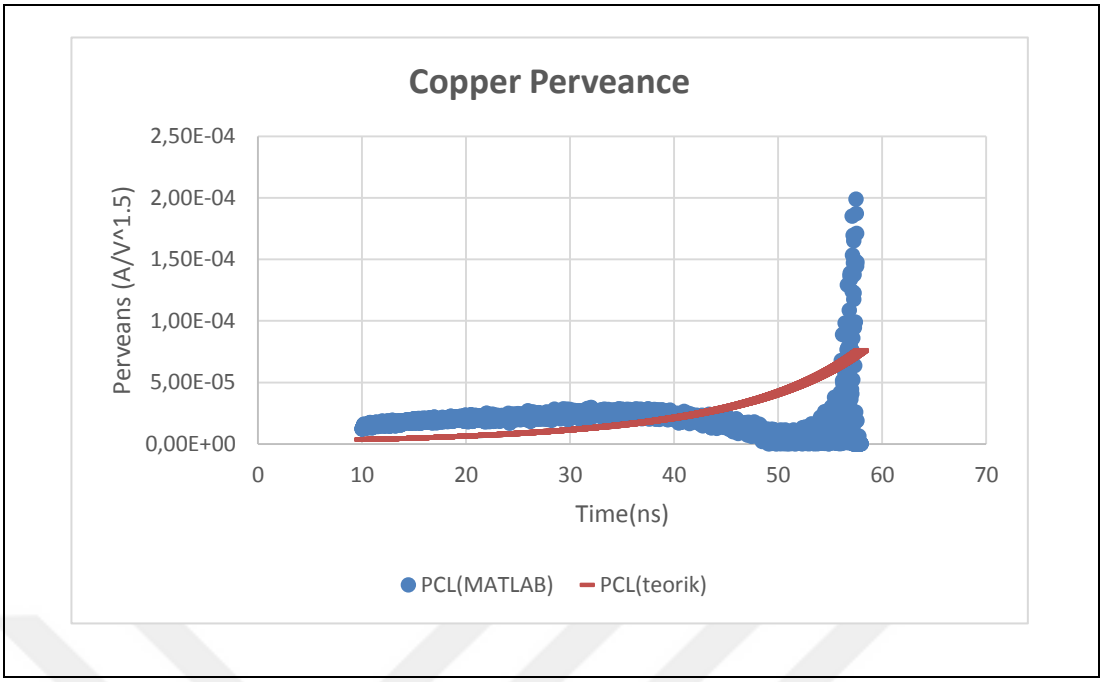

Figure 4.17: Copper Material Perveance.

The cathode radius used for simulations is 3.175 cm and the distance between the anode cathodes is 1.6 cm. The data in Table 4.2 is obtained together with the perveance calculations made considering these data.

Table 4.2: First Emission Percentage.

Materials	**PEC**	**Graphite**	**Aluminum**	**Copper**
v(cm/ns)	0.01496	0.013557	0.010233	0.017808
r_0(cm)	1.369133	1.712387	1.93485	0.793875
First Emission Percentage (%)	18,59532689	37,08816902	29,13702794	6,251968659

According to the values given in Table 4.2, the first area at the time of emission is the most graphite material. According to the experimental studies, graphite is the material with the highest percentage of first emission area except

velvet and carbon fiber. When the simulation results obtained are compared, we obtain the same result.

4.2. Testing the Vircator System in CST Simulation Environment

CST Particle Studio (PS) was used for electromagnetic and particle simulations. The physical parameters of the vircator used in the simulation are shown in Table 4.3 and the solid model plotted in Figure 4.18.

Table 4.3: Vircator Simulation Parameters.

Cathode radius	2 cm
Diode zone length	6.5 cm
Vircator zone length	20 cm
Voltage rating	290 kV
Anode-Cathode gap	0.5 cm
Drift Tube radius	4.8 cm

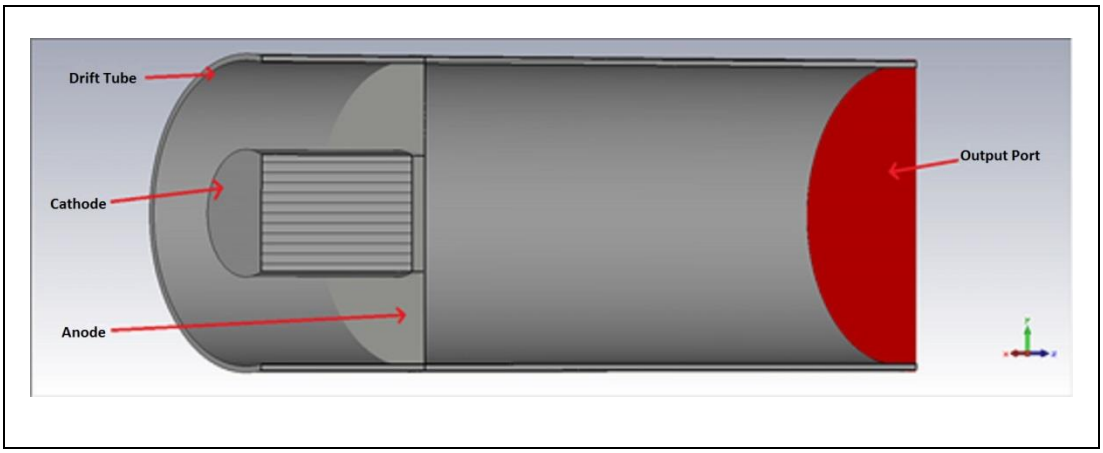

Figure 4.18: CST Vircator Model.

Figure 4.19 and Figure 4.20 shows the formation of the virtual cathode. The virtual cathode occurred approximately as far as the anode-cathode gap from the anode.

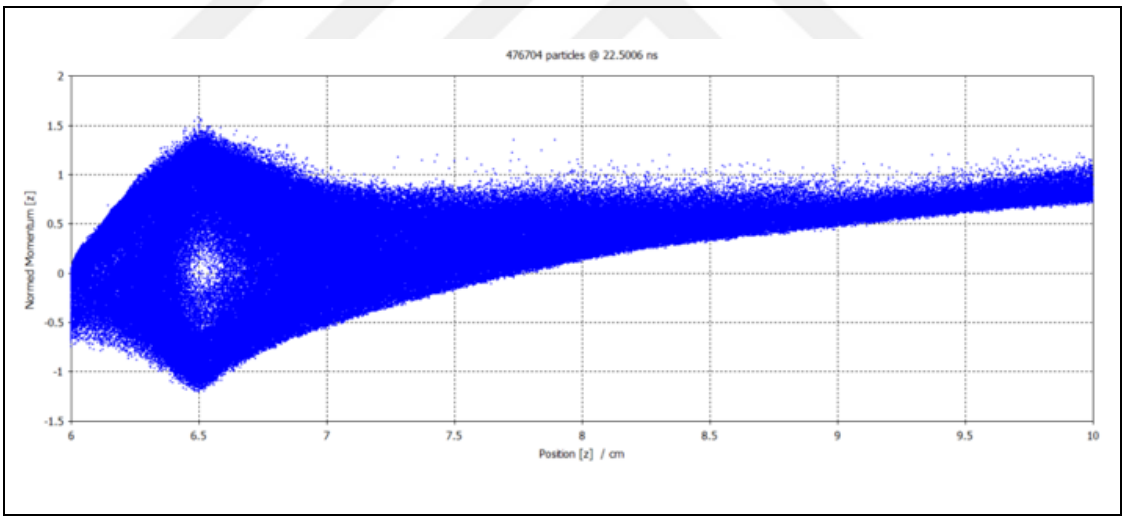

Figure 4.19: Formation of Virtual Cathode.

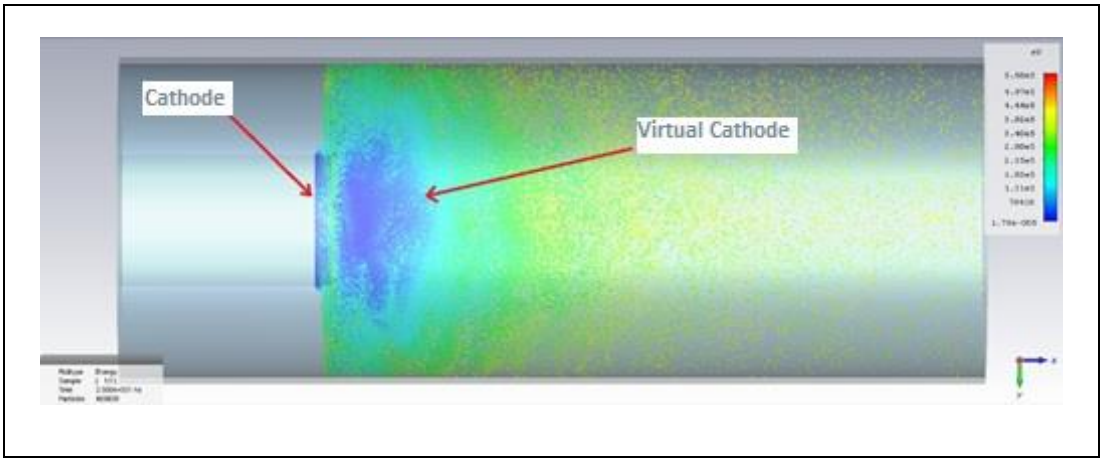

Figure 4.20: 3D Virtual Cathode View.

A current monitor is added to the simulation to measure the amount of current exiting the virtual cathode. Figure 4.21 shows the time-dependent current reading from the current monitor. The current generated by the virtual cathode is about 24 kA.

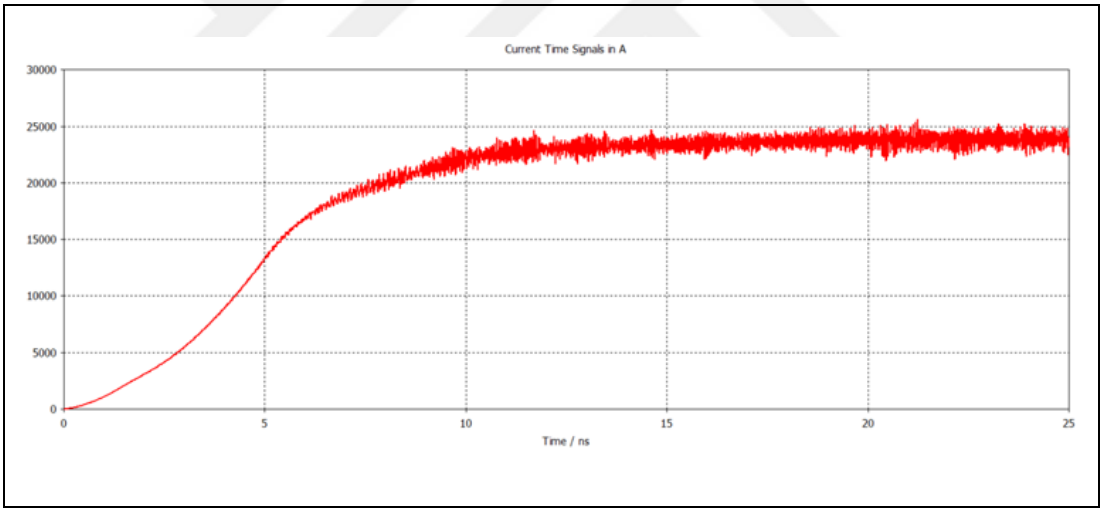

Figure 4.21: Variation of the current flowing through the virtual cathode over time.

To measure the electric field value from the virtual cathode, an electric field probe was added to the 9.5 cm distance from the anode. With the help of this probe, the variation of the electric field over time was examined. Then the frequency-dependent change of this signal by taking Fourier transform was also observed. These changes are seen in Figure 4.22 and Figure 4.23.

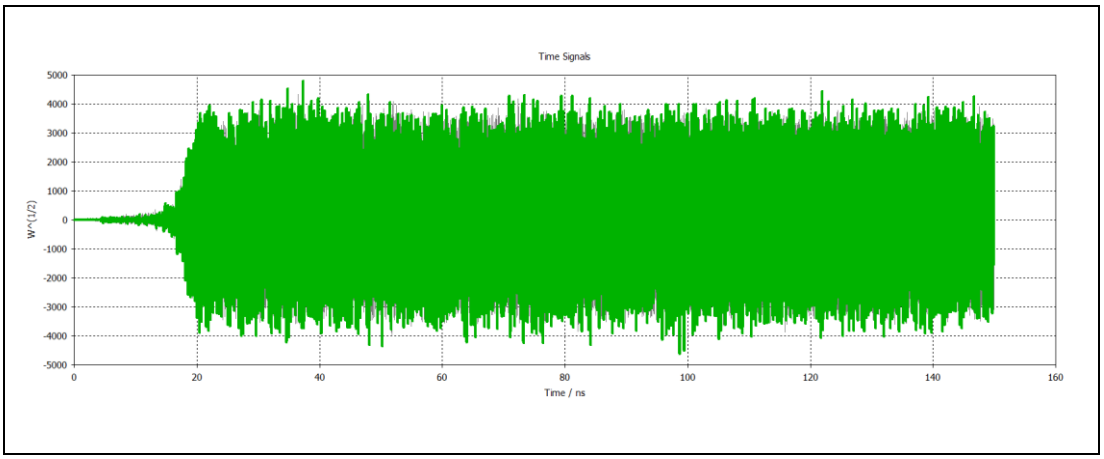

Figure 4.22: Variation of Electric Field Signal Over Time.

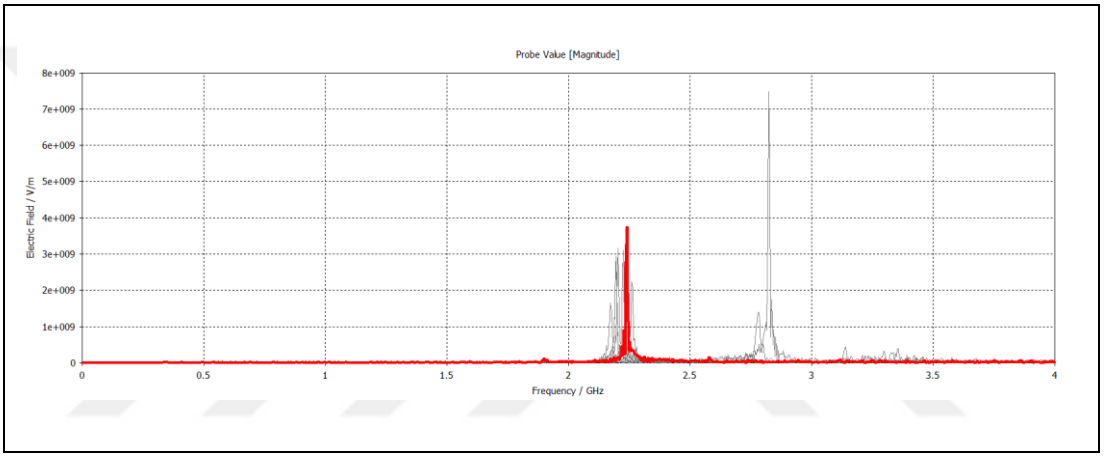

Figure 4.23: Frequency-dependent Variation of the Electric Field Signal.

The virtual cathode oscillator, designed as shown in Figure 4.23, operates in the 2-4 GHz frequency band. The electrons oscillating between the real and the virtual cathode by reflecting from the virtual cathode play an important role in the formation of high-power microwave. The distance between the anode and the cathode has an important role in determining the operating frequency of the vircator. The frequency-dependent graph of the distances between different anode cathodes is shown in Figure 4.24.

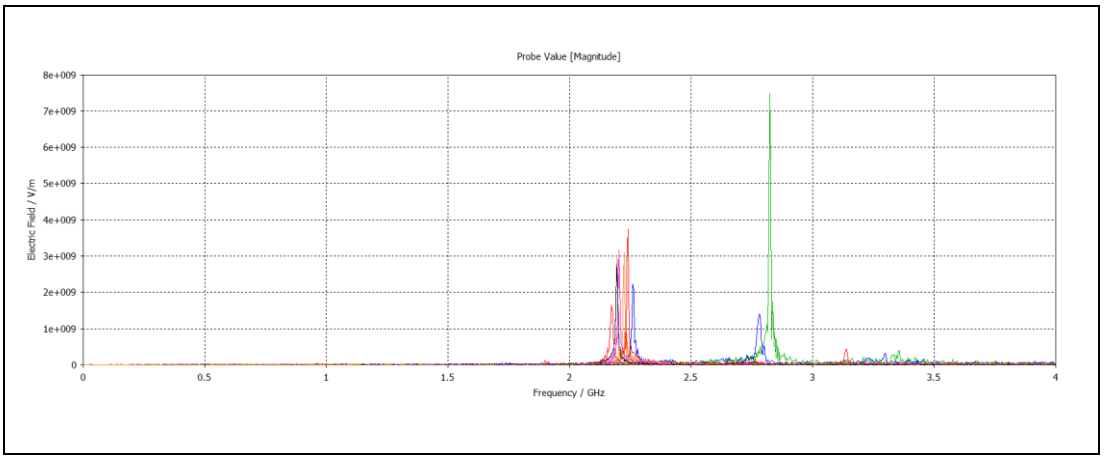

Figure 4.24: Frequency spectrum of different anode cathode distances.

Simulation studies have shown that as the distance between the anode cathode increases, the frequency of the microwave signal emitted from the vircator decreases.

4.2.1. Axial Vircator CST Simulations

The axial vircator is designed to avoid the problem of scattering the oscillation cloud over long distances in electron movements in the reflex triode vircator. In this type of axial symmetry, the electric field lines are smoother. The factors affecting the microwave output are only the voltage applied to the distance between the anode - cathode.

Multiple anode structures may be formed to increase the stability of the axial vircator. Electrons emitted in bunches provide stable frequency oscillation. The cavity between the two anodes is placed in the region around the virtual cathode. The resulting microwave becomes amplified.

In the axial vircator, the anode and cathode are parallel to each other and share the same central axis. Electron radiation is generally obtained from the cathode by negative feed. The general view of the axial vircator is given below:

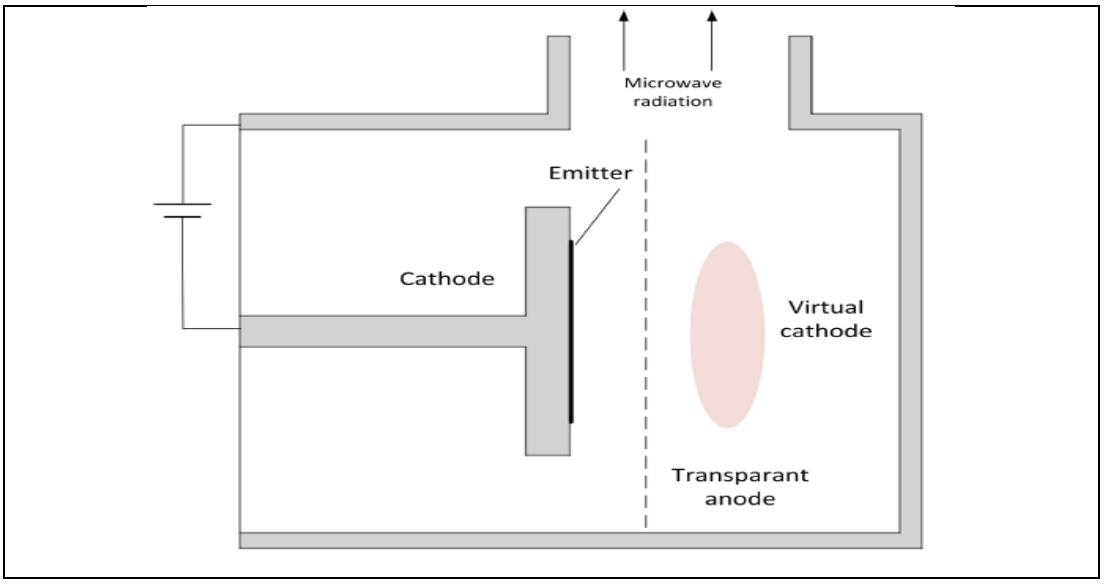

Figure 4.25: General view of axial vircator.

The positive aspects of the axial vircator are as follows::

- There is no deflection problem of the electron beam, as in the reflex triode vircator, the released electrons exhibit more stable behavior, factors affecting microwave output are only the distance between the anode and cathode and the voltage applied to the cathode.
- Operating principle is easier than other types of vircators and high-power microwave-producing devices.

Negative sides can be listed as follows:

- 5% or less efficiency.
- Anode-to-cathode distance adjustment is not easy (without breaking the vacuum).

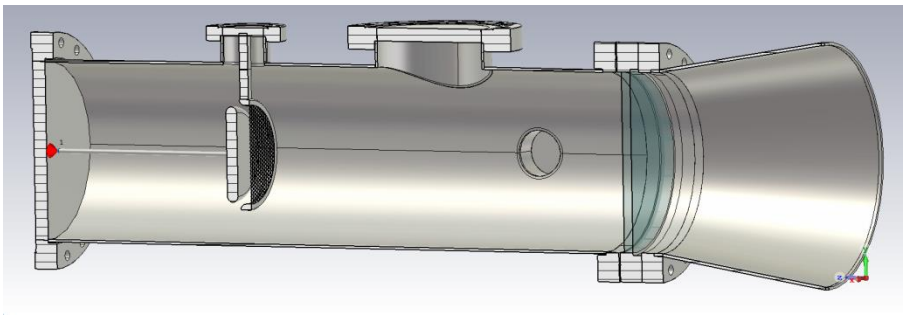

Figure 4.26: Axial Vircator CST Design.

Experimental studies with axial vircator and experiments in simulation environment are available. Of these, Weihua Jiang's [4] experimental studies were compared with the same experimental parameters that we made in the CST simulation environment.

The frequency values obtained according to experimental studies are observed in various band intervals. The maximum power obtained is ~ 10MW and the efficiency obtained is about 1% or less. All of these experimental data and vircator parameters are summarized and given in Table 4.4:

Table 4.4: Vircator Parameters.

Anode cathode distance [mm]	25
Anode transparency [%]	85
Vacuum tube length [mm]	1000
Vacuum tube radius [mm]	105
Applied signal duration [ns]	150

Table 4.4 (continued)	
Voltage applied to cathode [kV]	400
Cathode radius [mm]	60

Comparison of experimental results with CST simulation results:

In this article, microwave signal form measured with D-Dot probe and microwave signals obtained from CST PS are compared:

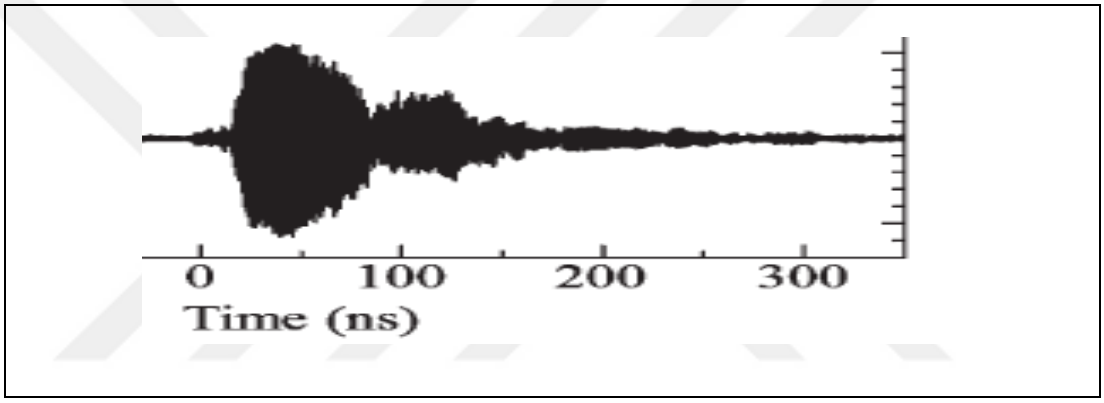

Figure 4.27: Signal Form in the Literature [4].

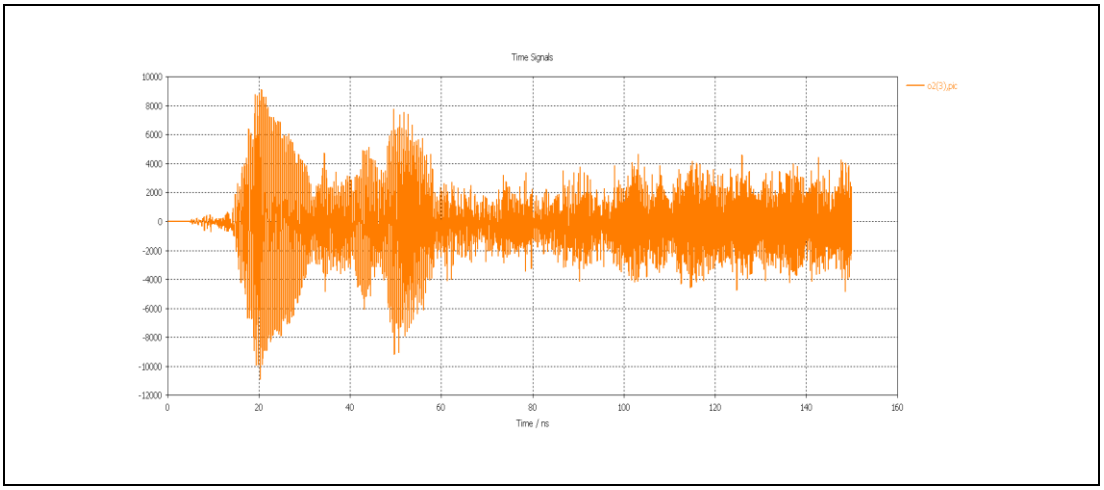

Figure 4.28: Signal form obtained from CST PS results.

If the Fourier transform is applied for both signals:

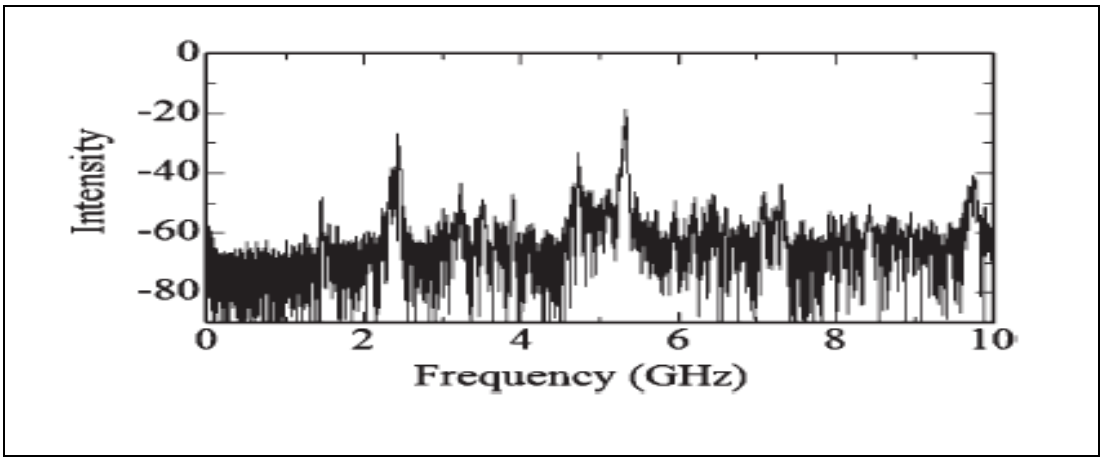

Figure 4.29: Literature results [4].

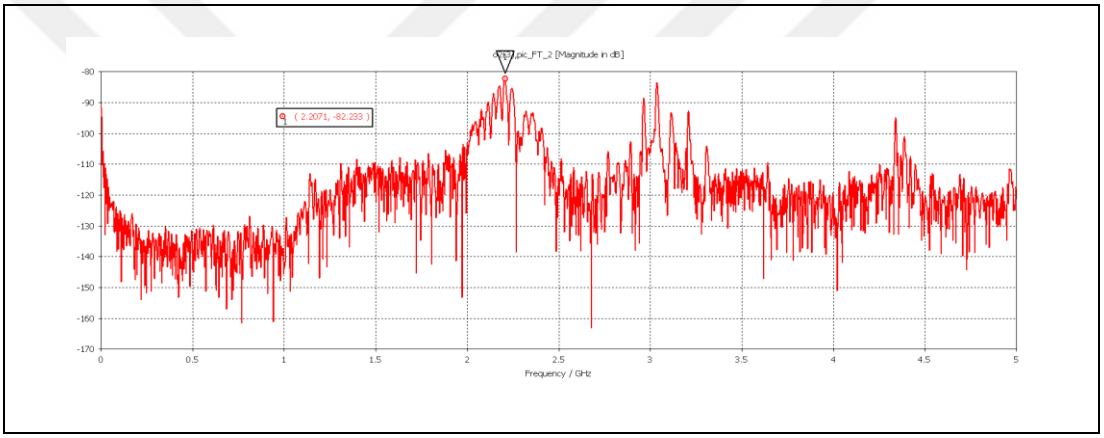

Figure 4.30: CST PS result.

When the results of the Fourier transform received signals in the frequency space are examined, results similar to those in the literature are obtained. As a result of the simulation studies, the space momentum graph of virtual cathode formation is obtained as follows:

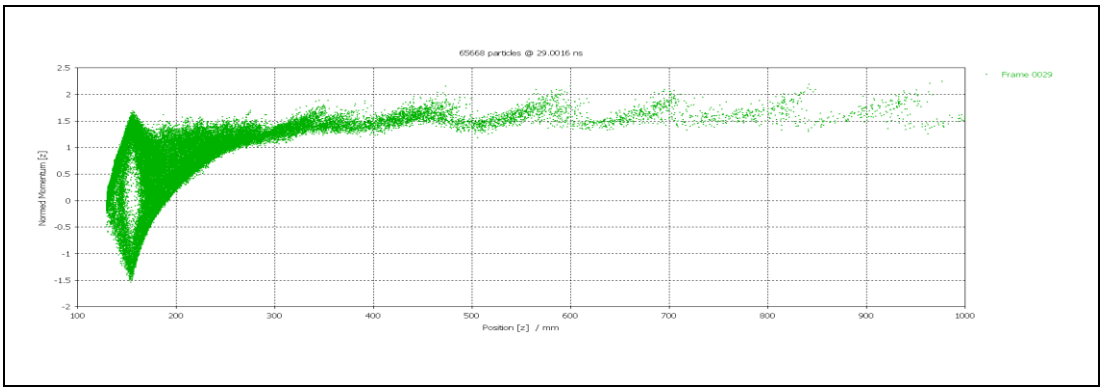

Figure 4.31: Space Momentum View.

When we examine the results of the simulation studies, it is seen that the frequency components have almost similar values in the measurement and simulation results. However, when the output power is compared, higher power values are obtained in the simulation studies.

Table 4.5: Comparison of Simulation Results.

	Experimental	CST PS
Output Current [kA]	13kA	20kA
Maximum output power [MW]	10	118
Dominant frequency [GHz]	2.4	2.2
Efficiency [%]	< 1	1.4

Although axial vircators are simple fabricable structures, their efficiency is low. Different methods are being tried to eliminate this problem. One of these is the multiple anode structures mentioned above. If more than one anode structure is used in axial vircators, more virtual cathodes will be formed. The number of electrons

entering the oscillation and the resulting electromagnetic wave will increase. Increasing the output power means that the efficiency of the vircator increases.

Experiments were performed in simulation environment for higher anode structure and higher efficiency was obtained compared to ordinary axial vircators. The figure below shows the 3D drawing of the multiple anode structure of the vircator and the resulting electron cloud virtual cathode distribution.

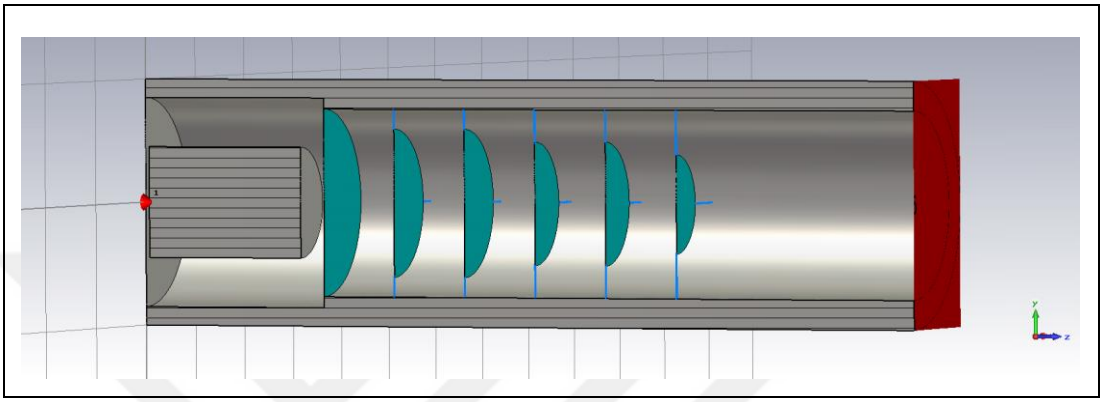

Figure 4.32: Multiple anode structure.

We have said that more than one virtual cathode formation will occur in multiple anode structures. The representation of electron movements obtained from simulation studies is given in Figure 4.33.

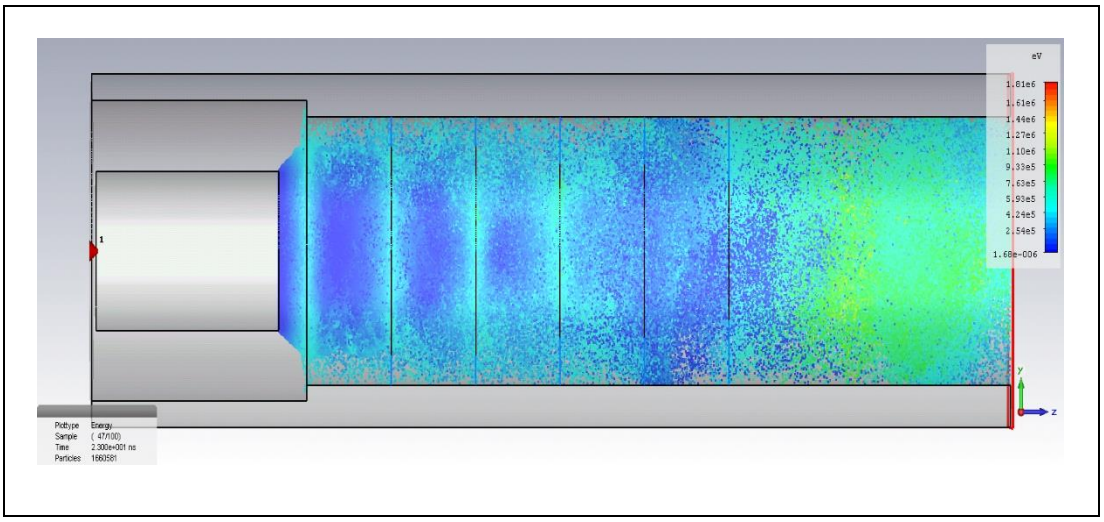

Figure 4.33: Virtual cathode formation.

When the results of the simulation studies are examined, the momentum distribution graph of electrons is given in Figure 4.34.

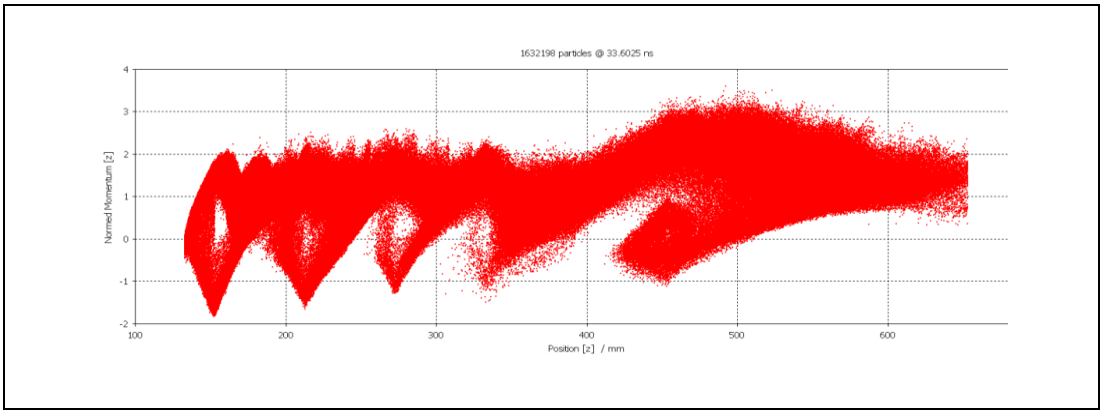

Figure 4.34: Space momentum distribution graph of electrons.

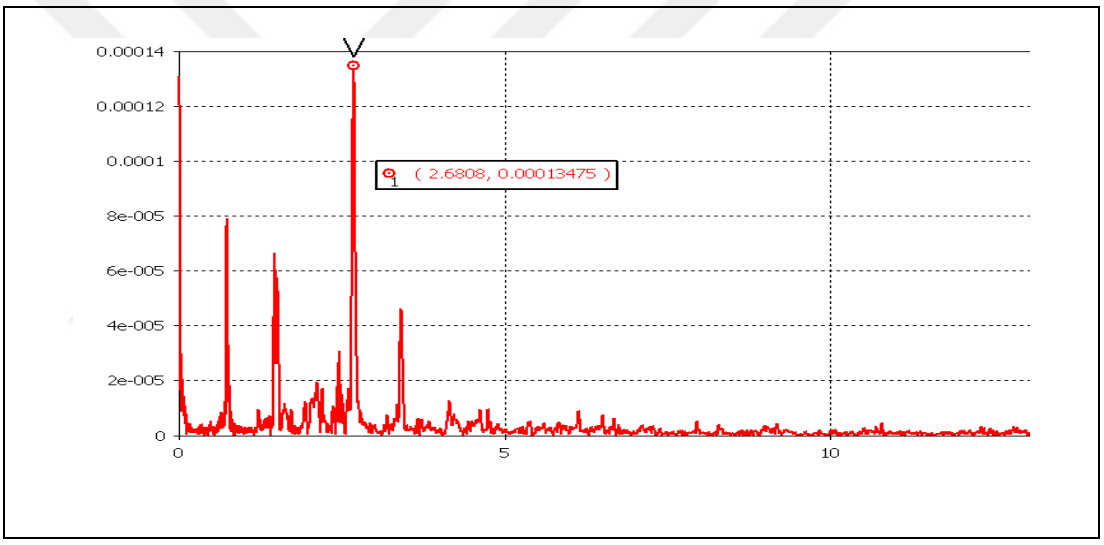

Figure 4.35: Frequency distribution of electrons.

In the study, the distance between the anode cathode is equal to the distance between all other anodes. All anodes have the same potential. Negative potential applied to cathode. Considering all these situations, the only difference from classical axial vircator is the use of multiple anode structures.

Table 4.6: Parameters used in simulations.

Anode Transparency	%70
Anode Radius (mm)	77
Cathode Radius (mm)	45
Anode - Cathode Distance (mm)	23
Acceleration Tube Length (mm)	500
Voltage (kV)	511

Table 4.7: Simulation results.

Output Power (MW)	127.75
Frequency (GHz)	2.68
Input Power (GW)	1
Efficiency (%)	8

As a result of the simulations, it is seen that the efficiency can be increased by using multiple structures in axial vircators.

4.2.2. Reflex Vircator CST Simulations

The reflex triode vircator is similar to the axial vircator model. The anode and cathode are positioned parallel to each other. Unlike axial vircators, the anode is excited by a positive pulse signal. The general geometric structure is as follows:

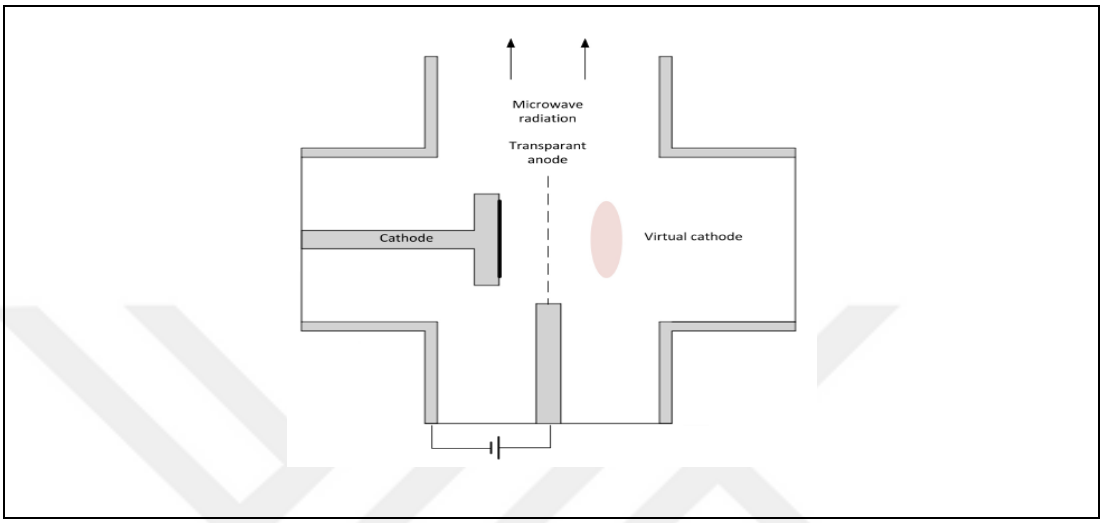

Figure 4.36: Reflex Vircator.

The positive sides of the reflex triode vircator are listed as follows:

- It is easier to change the geometry during the operation compared to other models of vircators. Particularly advantageous is that the anode cathode distance is adjustable.
- The efficiency value of other types of vircators ranges from 1% to 2%, 12% efficiency can be achieved in experiments with reflex triode vircator.

The negative aspects of the reflex triode can be written as follows:

- Since there is no cavity around the virtual cathode in this type of geometry, the output frequency value is not stable.
- When there is a cavity around the virtual cathode, the microwave radiation generated by the reflected electrons is perceived by the virtual cathode as the external magnetic field strength and forces the electrons in the virtual cathode to

oscillate at the same frequency. The path it follows is not linear, in this case electrons due to Lorentz force and this leads to energy losses.

Experimental studies with reflex triode vircators were compared with simulations with CST PS. The parameters for the test are summarized as follows:

Table 4.8: Reflex Vircator CST Parameters.

Anode cathode distance [mm]	15
Anode transparency [%]	70
Cathode radius [mm]	38.5
Vacuum tube length [mm]	400
Vacuum tube radius [mm]	200
Aplied voltage [kV]	300
Signal duration [ns]	300

In general, the geometric structure designed in CST PS environment is as follows:

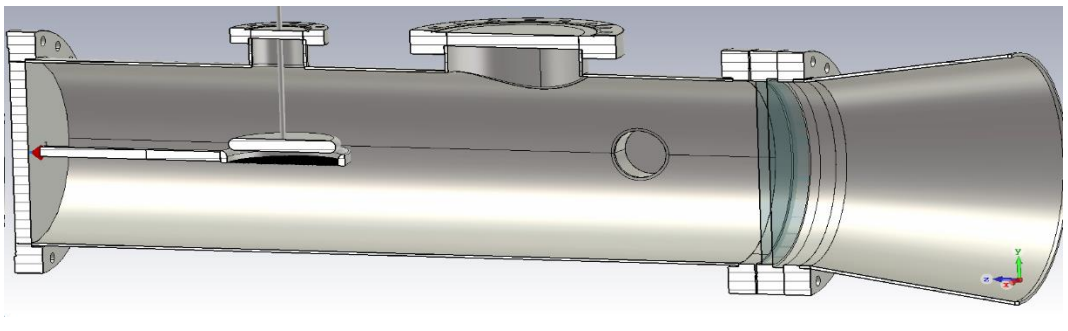

Figure 4.37: Reflex Vircator.

The momentum graph of the electrons obtained from the simulation results is as follows.

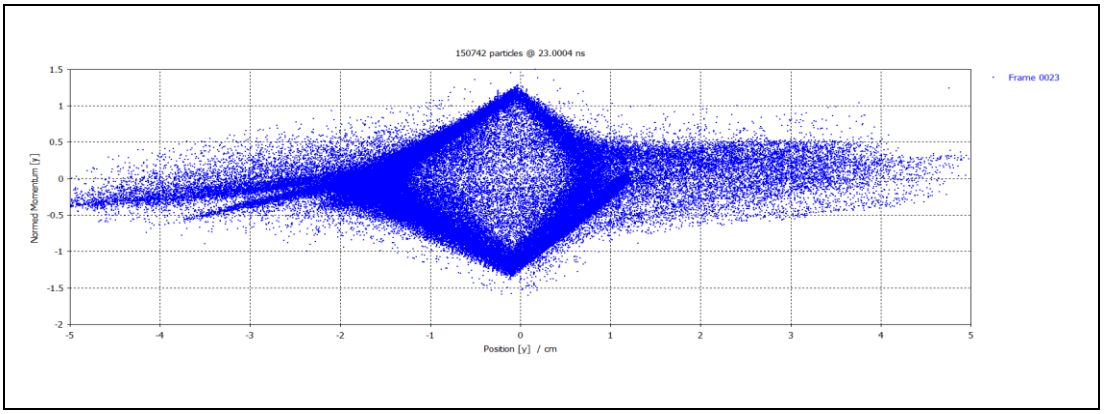

Figure 4.38: Reflex Vircator Virtual Cathode Formation.

The dominant frequency value was found to be 2.4 GHz according to experimental studies. The results obtained from CST PS show a frequency of 2.6 GHz. As it is seen in the figure below, microwave output frequency is spread to the band in reflex vircator structures unlike axial vircator.

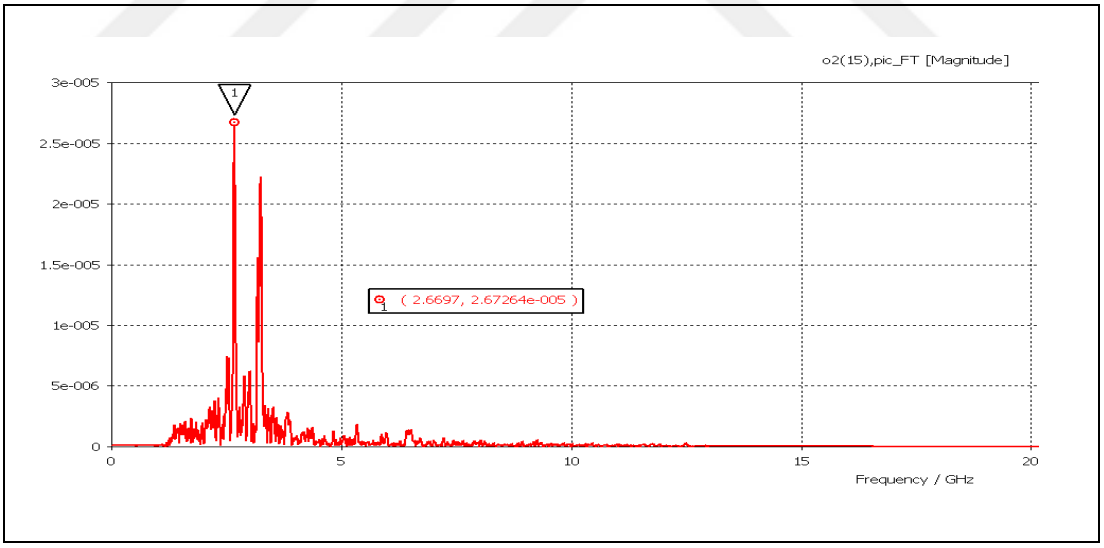

Figure 4.39: Reflex Vircator Output Signal Spectrum.

Table 4.9: Comparison of Results.

Experimental and CST PS simulation results comparison		
	Experimental	CST PS
Maximum output power [MW]	48	47.44
Dominant frequency [GHz]	2.4	2.6

Since there is no cavity in the reflex triode vircator geometry we investigated, the equation solutions of waveguide geometry are taken into consideration in order to determine the resonance modes formed by electrons. From these equations, it was calculated how far the cathode should be from the head of the vacuum tube. The distance is called the resonance distance:

$$\text{Resonant length (n,f)} = (2n-1)\frac{\lambda_{wg}(f)}{4} \tag{4.10}$$

$$\lambda_{wg}(f) = \frac{\lambda_{fs}(f)}{\sqrt{1-(f_c/f)^2}} \tag{4.11}$$

Where n is a positive integer, $\lambda_{wg}(f)$ wavelength in waveguide, $\lambda_{fs}(f)$ wavelength in free space and f_c is the cutting frequency of TE_{11} mode. Calculations were made from the interface prepared in MATLAB according to this equation set. After selecting harmonics according to n integer value, resonance distance is determined and required measurements are entered and results are obtained in CST

PS. The graph of the resonant length of the harmonics obtained according to the integer value n is as follows:

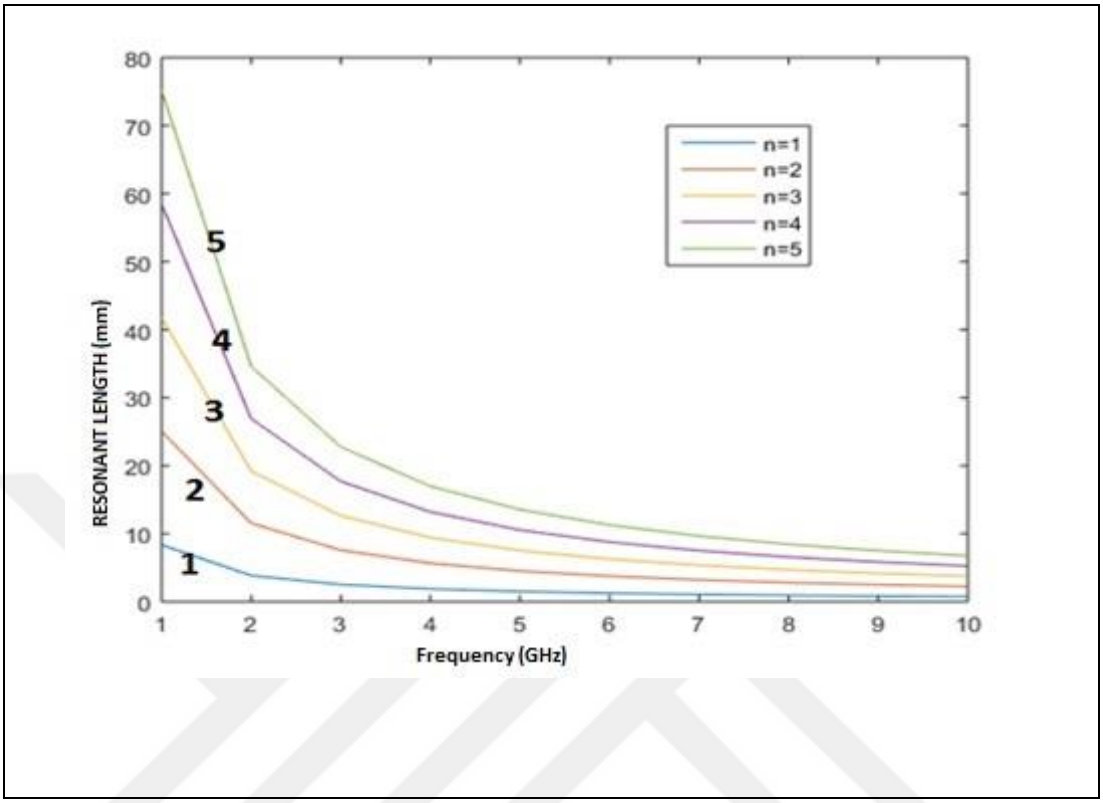

Figure 4.40: Resonant Length.

The resonance distance is as shown in the figure below.:

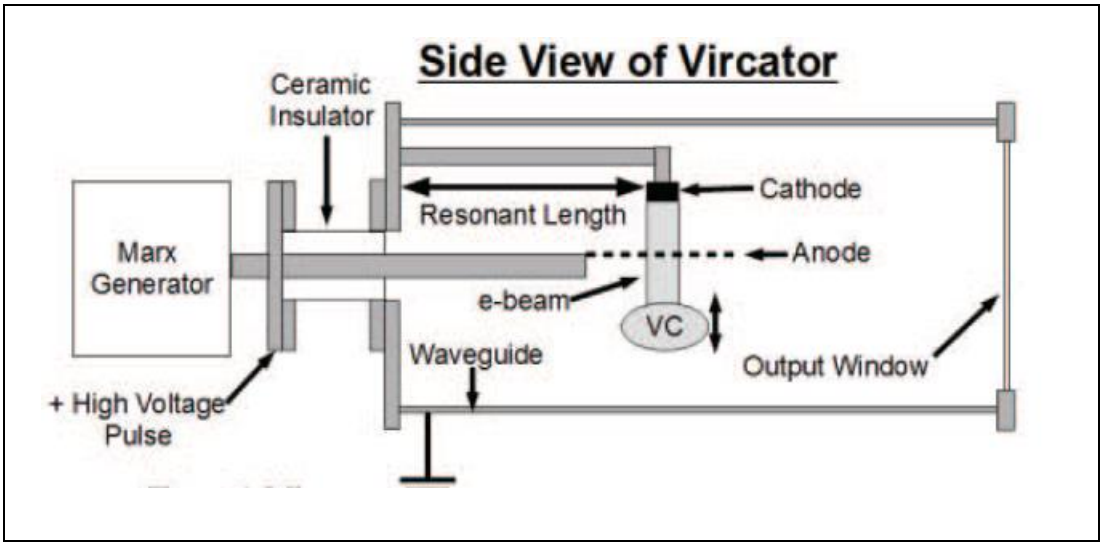

Figure 4.41: Resonant Structured Vircator.

Resonance distance calculation can be made with the program prepared using MATLAB.

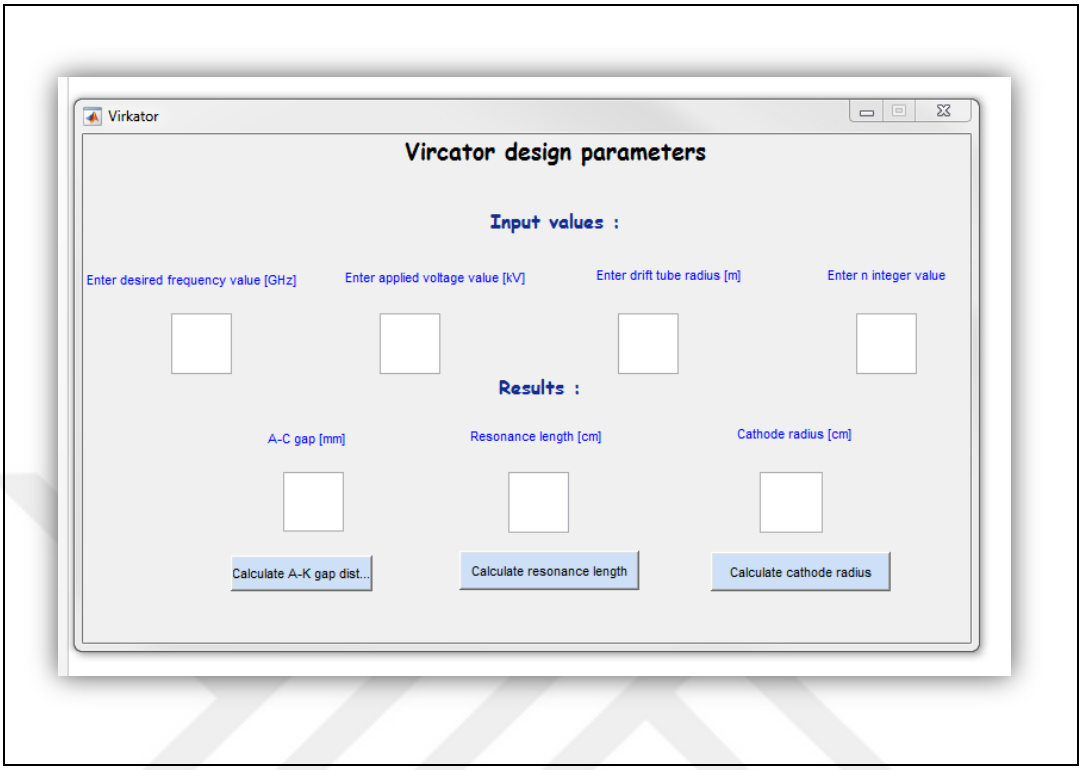

Figure 4.42: MATLAB program interface.

$$f \approx \frac{10}{12\pi}\sqrt{\frac{eV_{gap}}{md^2}}\ [Hz] \tag{4.13}$$

Anode-Cathode distance is calculated based on 4.13, independent of resonant length adjustment.

When the simulation results studies are performed according to the design of the calculated resonance distance of the vircator, it is possible to obtain a single frequency operating vircator in the reflex model. The Fourier transform of the microwave signal obtained from the CST PS gives the stable frequency value of the resonated electrons. The frequency obtained as a result of the studies can be seen in the graph below.

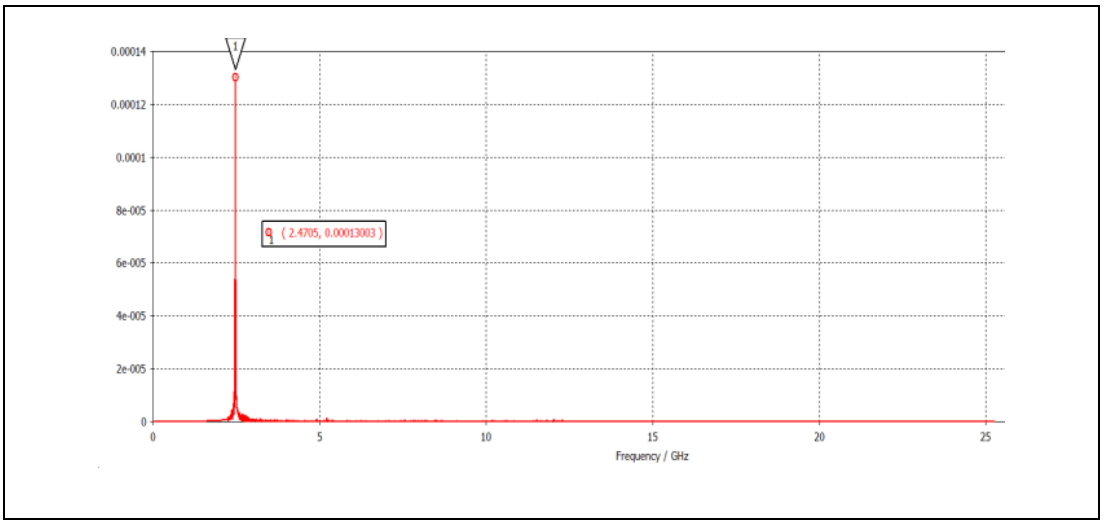

Figure 4.43: Resonant Length Adjusted Vircator Model.

5. TEST AND MEASUREMENTS

5.1. Vircator System Testing Environment

Infrastructure of KAMTAM building, which is located within TÜBİTAK-BİLGEM, was used for test and measurement studies.

Figure 5.1: Prototype of Vircator System.

The production of the vircator model, which emerges from the simulation studies and literature studies, is realized and placed in the laboratory environment as shown below. The high amplitude electrical signal generated in the Marx generator is transferred into the vacuum using a feedthrough. The anode and cathode structures in the vacuum are positioned in accordance with whichever reflex or axial vircator model is to be tested. In the axial vircator, the negative pulse is applied directly to the cathode electrode, while in the reflex model the positive pulse is applied to the anode electrode. In this way, a potential between the anode cathode is created to eject the electron..

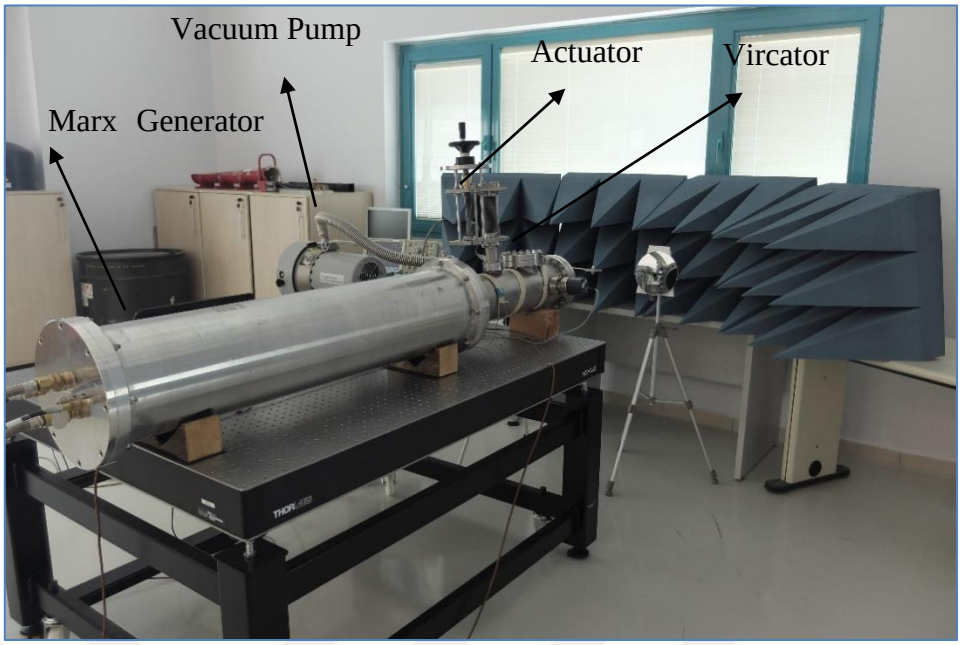

Figure 5.2: Vircator Test Assembly.

Vacuum level is critical in vircator systems. After the electrons are separated from the cathode, they need to interact with other molecules as little as possible in order to continue their path. For this reason, a turbo molecular pump is used to adjust the vacuum level. And vacuum level set to 10^{-5}~10^{-6} Torr levels. Another important issue in vircator systems is to adjust the anode cathode distance. Precise movement mechanisms are used to adjust this distance. In our system, a linear motion mechanism called actuator with micrometer sensitivity is used for this work. With the help of the actuator, the anode cathode distance was adjusted to the desired value and microwave signals in the appropriate frequency band were obtained.

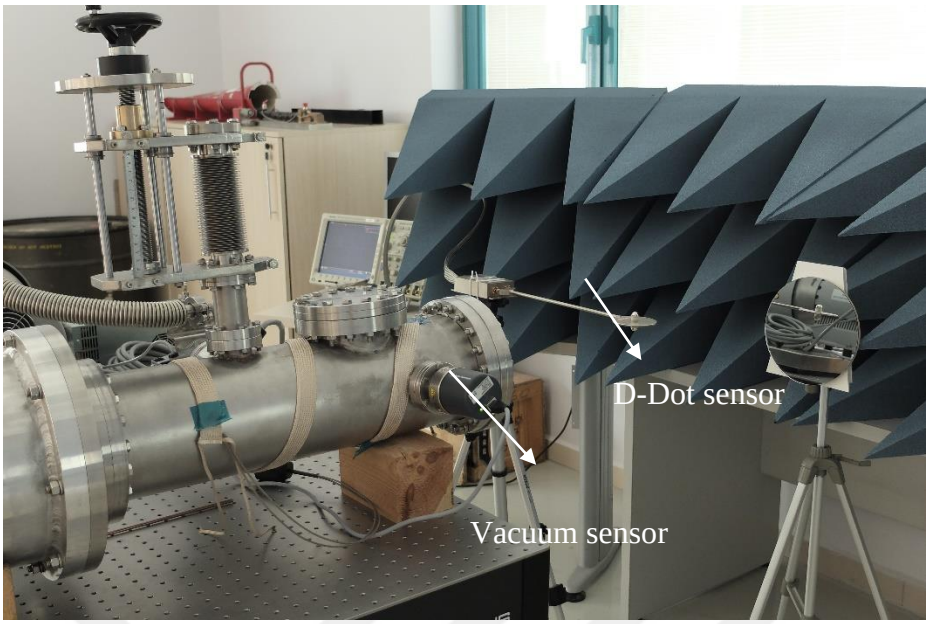

Figure 5.3: Vircator System Sensors.

As can be seen in Figure 5.3, vacuum level control can be monitored during operation by means of vacuum sensor on the vircator. In this way, materials which disturb the vacuum level in the vacuum chamber during the operation can be detected. Materials that are not suitable for the vacuum environment can be replaced with more suitable materials after the operation. Another sensor shown in Figure 5.3 is the D-dot sensor. This sensor is commonly used for measuring electric fields. The attenuated signal can be observed with the oscilloscope. The mirror is located in front of the camera to monitor plasma formation. Electrons are removed from the cathode by applying the electrical pulse. Since these electrons are eject by a very high electric field (especially from the pointed parts of the cathode material), they emit at high temperatures and in the form of plasma, not in the form of an electron beam, but as a dense electron-ion cloud. Some of these electrons passing through the grid anode form the virtual cathode after passing the anode approximately the anode cathode distance and electrons that pass through this cloud stream will reflect and return from here. Thus, the oscillation of this cloud causes high-power microwave propagation. Plasma formation part of this phenomenon for axial and reflex models was recorded with camera and mirror as in Figure 5.4.

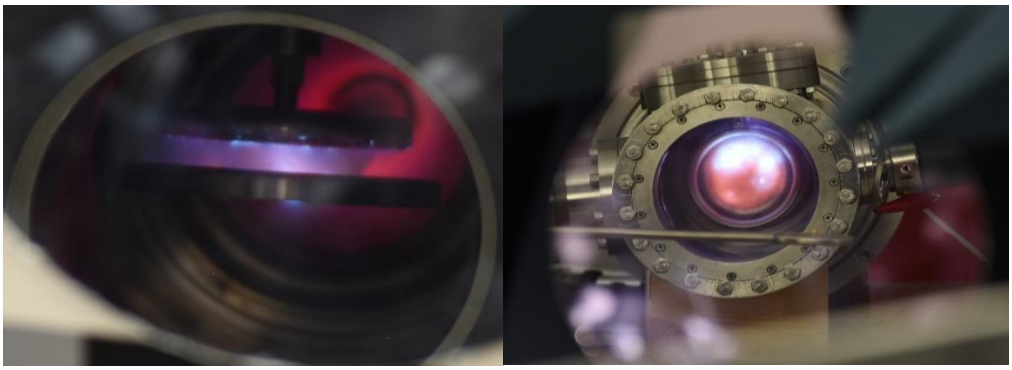

Figure 5.4: The image of the plasma formed in the vircator with the camera.

The smoothness of the plasma present here influences the operating power and efficiency of the vircator due to its reproducibility from every point of the cathode.

The results of various impact analyzes with computers are shown in Figure 5.5. The screen turns off completely after the computer is in operation and exposed to electromagnetic waves. This effect was also tested at different power and distance values and impact tests were recorded. It has been observed that the Vircator completely disables the computer from a maximum distance of 5 meters.

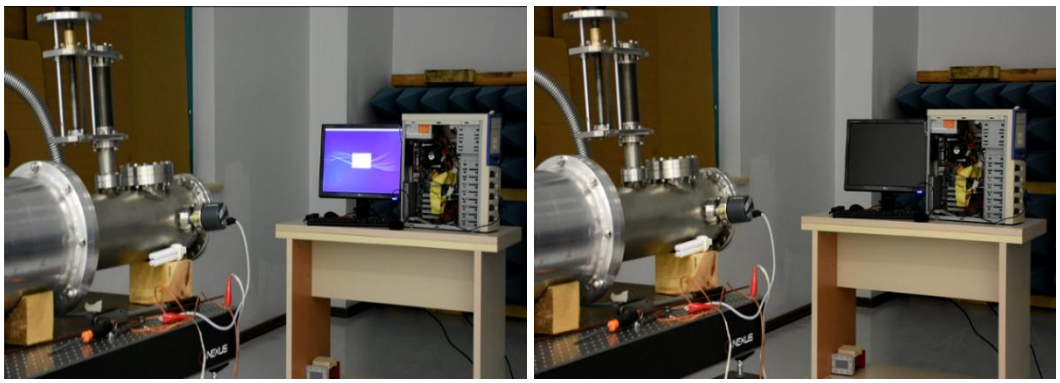

Figure 5.5: Before and After Impact.

5.2. Evaluation of Vircator Measurement Results

Measurement studies of the completed vircator were carried out in KAMTAM infrastructure within TUBITAK-BILGEM. Measurements were performed using a

D-dot probe. D-dot probes perform the measurements by taking the time-derivative of the electric field. The voltage at the output of the probe is given by the following formula:

$$V = RA\frac{dD}{dt} \tag{5.1}$$

Where R is the characteristic impedance, A is the equivalent field of the probe, and D is the displacement of the electric vector.

The vacuum level of the vircator system was adjusted to 10^{-5}~10^{-6} Torr levels by turbo molecular and mechanical pumps. The high amplitude electrical signal from the Marx generator was sent to the vircator. The transmitted signal form is shown in Figure 5.6.

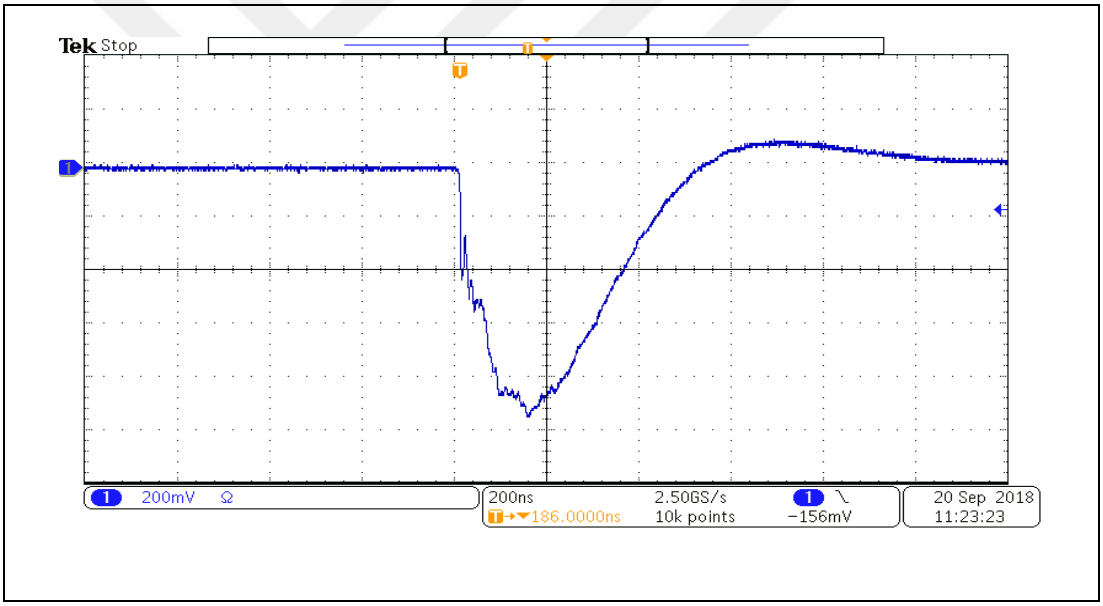

Figure 5.6: Marx Generator Output Signal.

The signal form shown in Figure 5.6 is a type of termination load called a water load with a copper sulfate solution. The impedance of the water load is obtained by connecting the harmonious load, which is almost identical to the output of the Marx generator. The signal generated at the load resistance was read through the oscilloscope by passing the signal over the 30dB attenuator. The compatible load, known as the water load, is shown in the following figure.

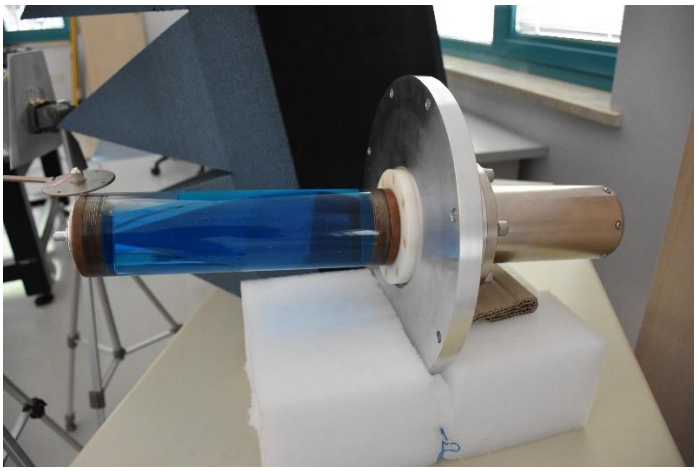

Figure 5.7: Water Load with Copper Sulphate Solution.

The element in Figure 5.8 is connected directly to the Marx generator instead of the vircator. In this way, the signal produced was checked before being sent to the vircator system.

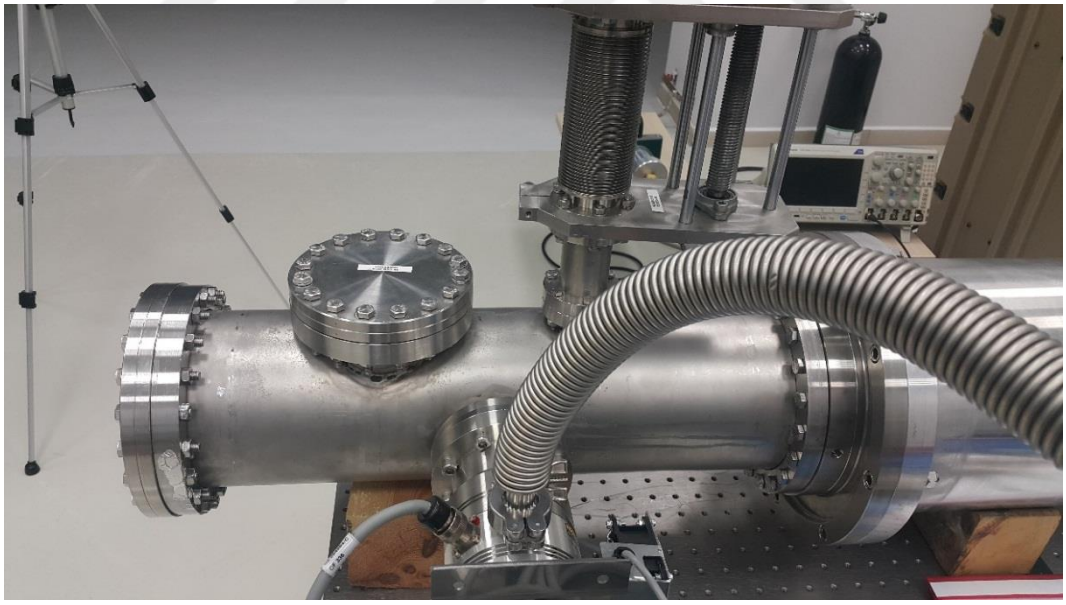

Figure 5.8: Final State of the Vircator System.

Thanks to the output signal of the Marx generator sent to the system shown in Figure 5.8, microwave signals were generated by the movements of electrons

detached from the cathode. The signals collected by the oscilloscope were processed in the Matlab program and interpreted. The oscilloscope data obtained from measurements taken at a distance of 5 m is shown in Figure 5.9.

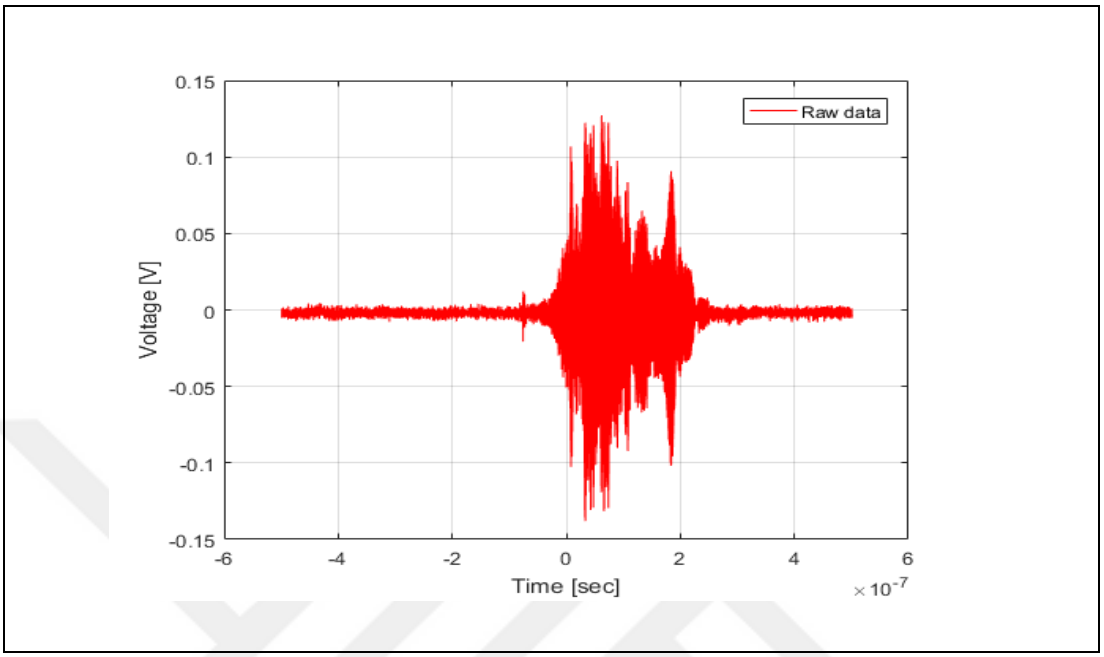

Figure 5.9: Raw Oscilloscope Data

When the results obtained from the Vircator are examined, signals below 100 MHz cause excessive noise in the processing of the data. Signals below 100 MHz, however, are not significant signals for the vircator system. In the Matlab program, clean data was obtained when a filter was applied below 100 MHz frequency. Filtered data were processed in Matlab program and electric field values were calculated. The results obtained are shown in Figure 5.10.

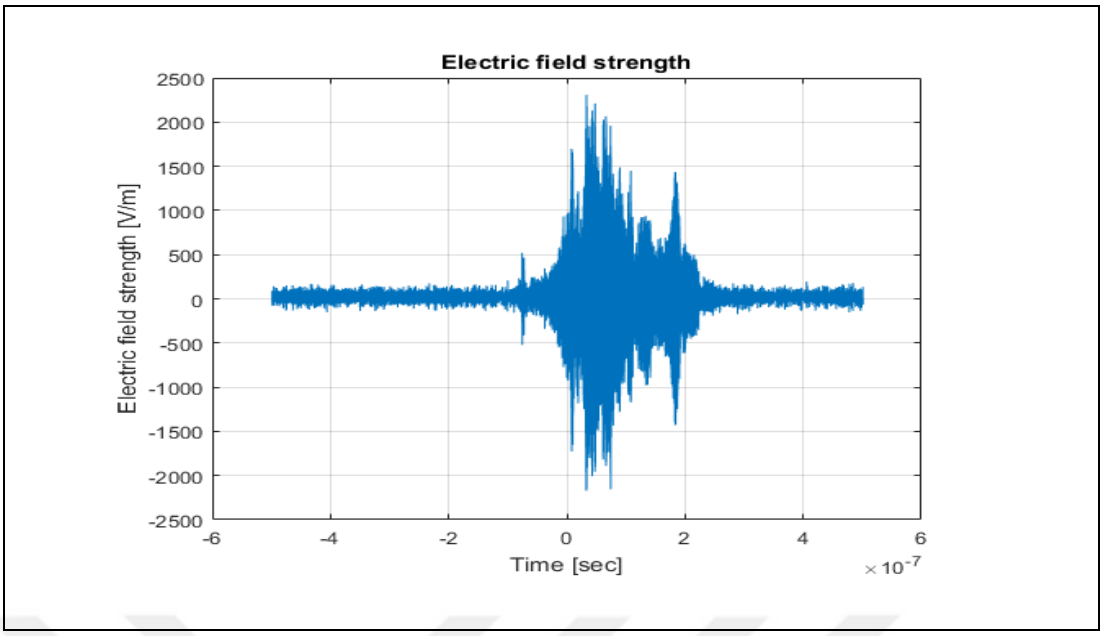

Figure 5.10: Electric Field Values.

The frequency range of the output of the vircator was determined by applying foruier transform to time dimensional electric field change. As shown in Figure 5.11, the main operating modes of the vircator are 3.7, 4 and 4.3 GHz. However, the highest amplitude appears to be 3.7 GHz.

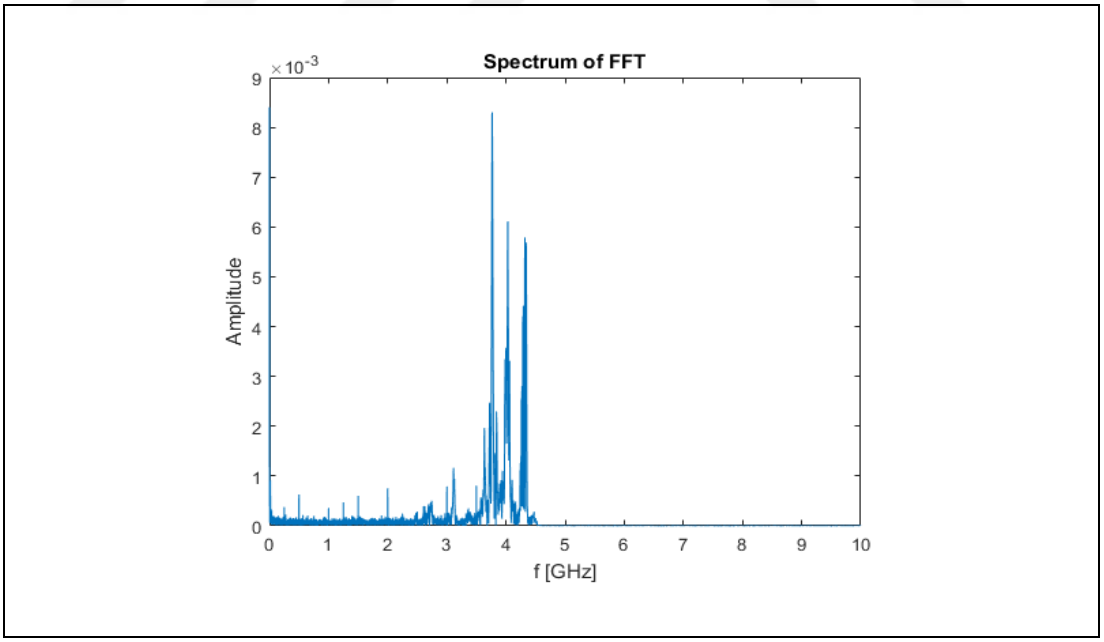

Figure 5.11: Fourier Transform Applied Data.

When the results obtained in our system are examined, our target frequency band is selected between 2-4 GHz. In this context, without changing the applied voltage (200 kV), if we increase the anode cathode distance from 8 mm to 10 mm, the results obtained from the same distance are as follows:

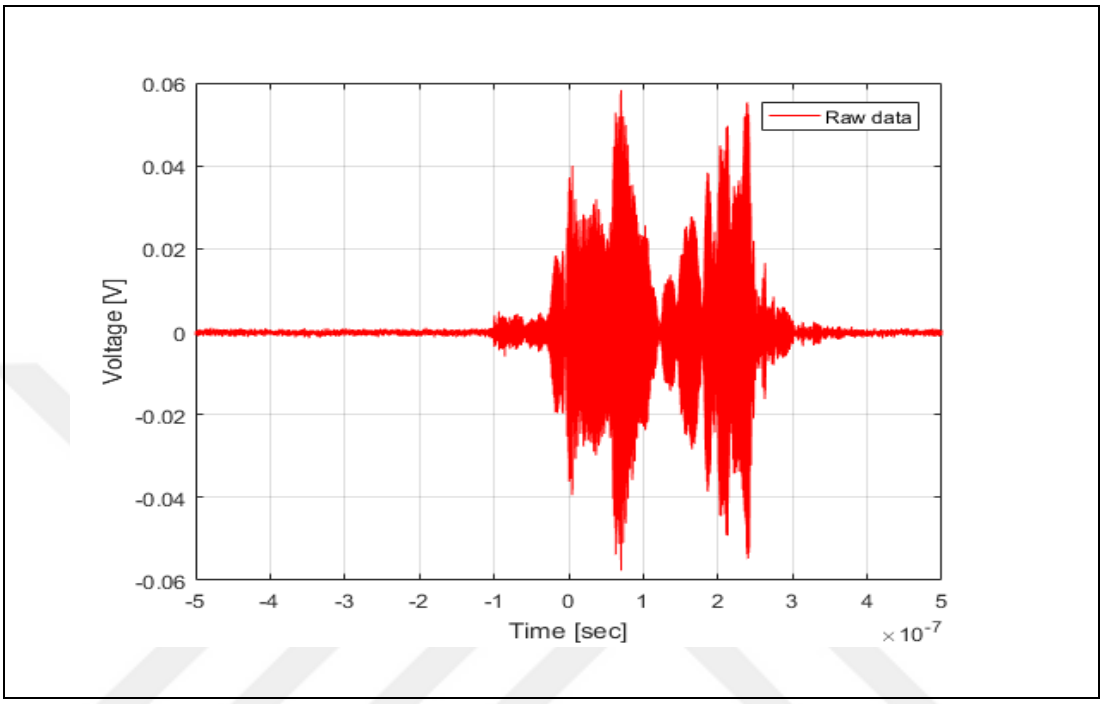

Figure 5.12: Raw data for 10mm AK distance.

After applying the noise correction we applied for the previous results to this signal, when we analyzed the signal we obtained with MATLAB program, the corresponding amplitude values in the electric field and frequency space were as follows.

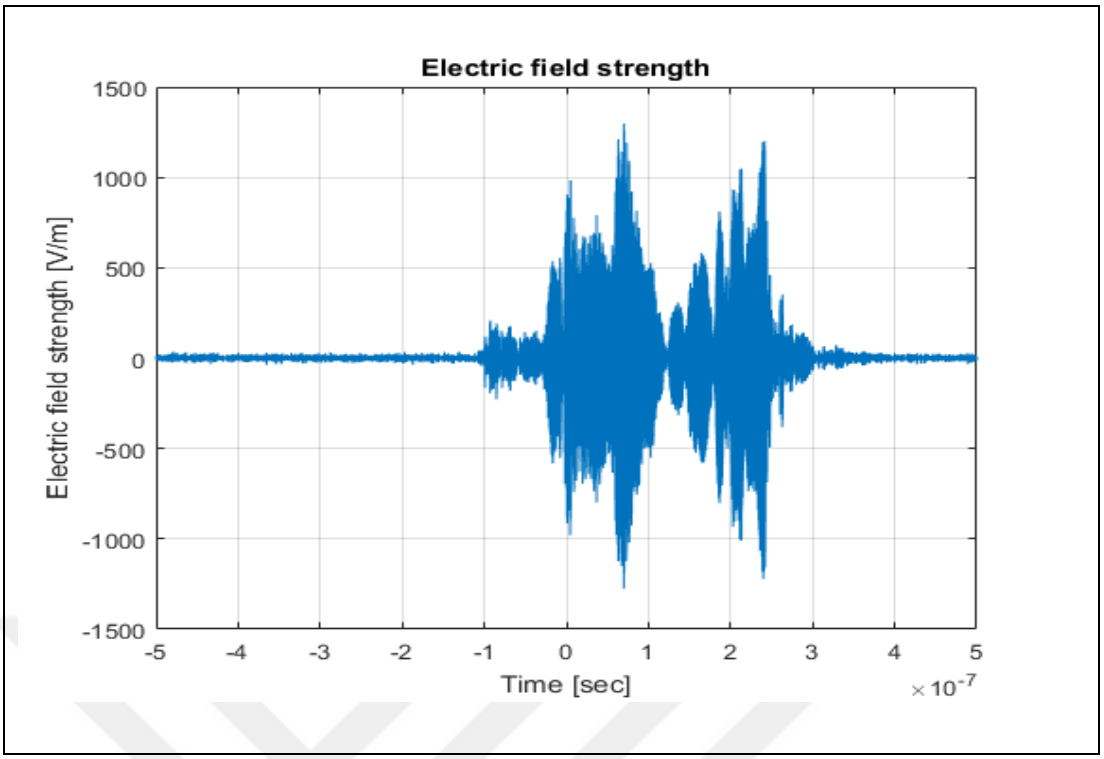

Figure 5.13: Electric field value for 10mm AK distance.

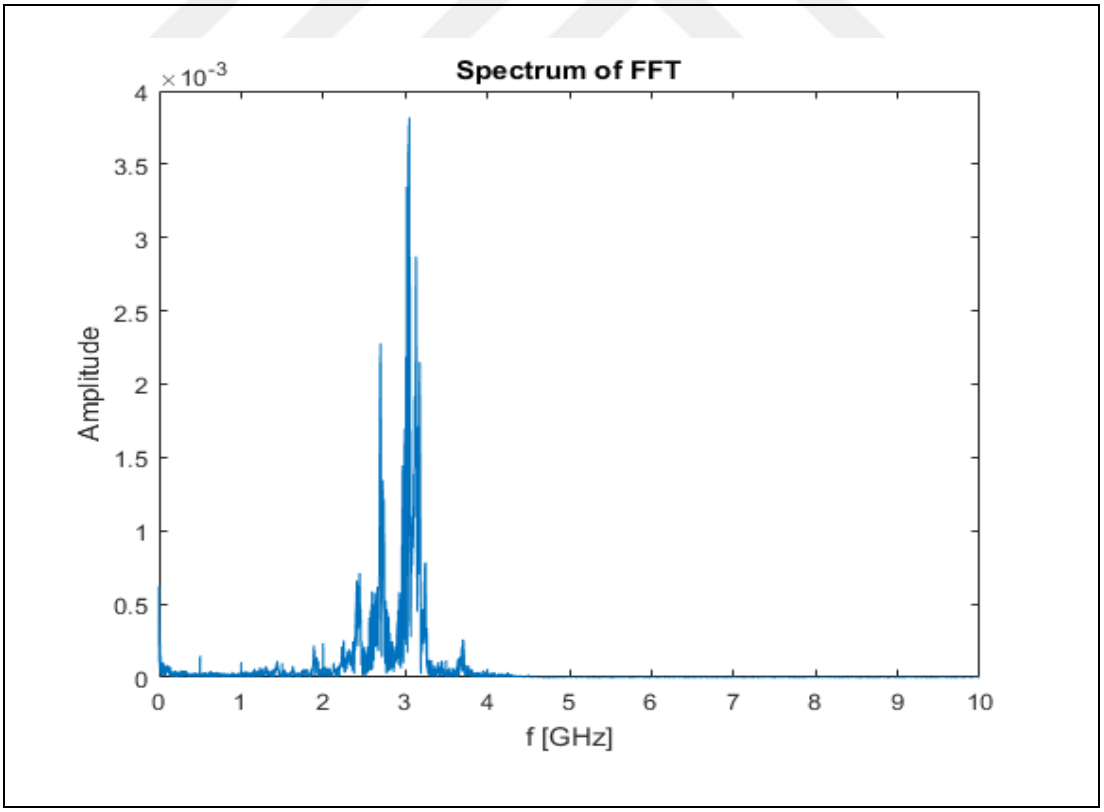

Figure 5.14: S Band Vircator Output Spectrum.

As shown in Figure 5.14, the desired frequency values can be adjusted by changing the anode cathode distance in the vircator systems. In addition, an increase in anode cathode distance can result in lowering the power band and lowering the frequency band to lower values. As can be understood from this, as in theory, the anode cathode distance and frequency value are inversely proportional.

6. CONCLUSION

In this thesis, a system which is used to produce high power electromagnetic signals and called as vircator is investigated. Studies have shown that the vircator is a system that is easier to produce and use than other microwave sources to produce high-power signals. However, low productivity is a matter that needs to be studied. In order to solve this problem, many different applications can be done as seen in the thesis. Improving the anode structure and testing different materials for the cathode are some of them.

In the thesis, graphite was first used for cathode structure and electromagnetic signals were collected. However, when we change the cathode structure to velvet, much more regular and higher electromagnetic signals are obtained. The reason for this is that the very thin and sharp points on the velvet make it easier for the electric field value to reach higher values at these points. This increase in the electric field value at the ends also contributes to the easier removal of electrons. The increase in the number of electrons entering the vacuum zone has led to a more stable formation of the virtual cathode and thus increased microwave production. This chain effect was observed by the use of velvet cathode.

Anode production is also critical for the vircator. Attention was paid to adjusting the transparency ratio of the anode to around 70%, to ensure that the anode material does not poison the vacuum environment, that the thickness is adjusted correctly and that the gaps are about 1/3 of the anode cathode distance. Anode transparency is an important criterion for electrons to pass through the anode structure. However, when the anode transparency ratio starts to take values above 80%, it causes performance decreases instead of increasing the efficiency of the vircator. The reason for this is that the electrons passing through the anode region cannot interact with the anode sufficiently. Another important consideration for the anode is the type of material used. The anode material should be selected from the material that will not change the vacuum environment during the operation. Nickel, molybdenum and steel materials are recommended for this purpose. In our own system, we used stainless steel because it is easy to manufacture and easy to find.

When our results were examined, it was seen that steel material did not decrease vacuum level and it is a suitable material for our vircator system with its durability.

During the studies, two important factors were observed as voltage and anode cathode distance. Anode cathode distance can be adjusted according to desired frequency. However, this distance can be easily adjusted in the reflex model, while the axial vircator takes a long time to change this distance. To change the distance, the vacuum pumps must be switched off and the flanges opened. This situation causes long time loss in repeated studies. The voltage value can be easily adjusted from the Marx generator to the desired value. In order to reach higher powers, Marx generators with higher output power are needed.

Another important issue is the transmission of the signal from the Marx generator to the vircator without degradation. Here, a transition element called feedthrough is used which is resistant to high power and provides transition to vacuum environment. The impedance of this element is specially produced according to the output of the Marx generator. If the Marx generator is replaced and a different Marx generator is used, it must be replaced in this device. In the case of impedance mismatch, the signal is distorted before it reaches the vircator and cannot drive the vircator cathode. The produced vircator was specially designed and produced with feedthrough compatible with the impedance of the Marx generator.

All of these situations were simulated in CST-PS simulation environment and solved analytically using Matlab program. As a result of the simulation and mathematical analysis, the desired vircator system was produced and its measurements were completed.

7. FUTURE WORKS

In general, their efficiency is low. This was also observed during the thesis studies. There are studies to increase productivity in the literature. In the thesis, solutions for increasing productivity are mentioned in the simulation studies section. One way to improve efficiency is to use cavity structures within the vacuum zone. These structures increase the electromagnetic wave interactions and increase the electromagnetic power at the output. Another work on efficiency is to increase the electron emission of the cathode. For this purpose, the cathode surface can be treated with special methods or different coating techniques can be used to facilitate electron emission.

Marx generators are also of great importance in vircator systems. By using higher power Marx generators in the system and adjusting the signal at the output of these generators properly, more powerful vircator systems can be produced.

In order to increase the output power, antenna structures are used in the output of the vircator in the literature. The antennas can be used to direct electromagnetic pulses at the output and increase the power with the advantages of their gain. In future studies, it is aimed to produce more efficient and more powerful systems by considering these developments in vircator structures.

REFERENCES

[1] Mankowski J.J., (2015), "Solid Metal Cathodes for a Virtual Cathode Oscillator", Center for Pulsed Power and Power Electronics, Deparments of Electrical & Computer Engineering and Physics, Texas Tech University.

[2] Chen Y.J, (2005), "Compact, Repettitive Marx Generator and HPM Generation with the Vircator", Master Thesis, Texas Tech University.

[3] Davis A. H., Fulton R. D., Sherwood E. G., Kwan T. J. T., (1990), "Enhanced-Efficiency, Narrow-Band Gigawatt Microwave Output of the Reditron Oscillator", IEEE Transactions on Plasma Science, 18 (3), 611-616.

[4] Nagao K., Takatsu W., Thuan P. V., Sakurai K., Ashizawa W., Kuno H., Sugai T., Jiang W., (2018), "Characteristic Evaluation and Optimization of Virtual Cathode Oscillator with High Transmittance Anode", 15th Anuual Meeting of Particle Accelerator Society of Japan, 7-10 August 2018, Nagaoka,Japan.

[5] Woolverton K. S., (1998), "High-Power, Coaxial Vircator Geometries", Doctoral Thesis, Texas Tech University.

[6] Efremov A. M, Kitsanov S. A, Klimov A.I., Korovin S. D., Kovalchuk B. M., Kurkan I. K., Kutenkov O. P., Loginov S. V., Pegel I. V., Polevin S. D., Zherlitsyn A. A., (2001), "S-Band Vircator with E-Beam Premodulation Based On Compact HV Pulser with Inductive Energy Store", Instute of High Current Electronics SD RAS

[7] Polevin S. D., Efremov A. M, Zherlitsyn A. A., Kitsanov S. A , Klimov A.I., Korovin S. D., Kovalchuk B. M., Kurkan I. K., Kutenkov O. P., Loginov S. V., Pegel I. V., (2001), "S-Band Vircator with Electron Beam Premodulation Based on Compact Inductive Energy Storage Generator", Instute of High Current Electronics SD RAS.

[8] Kitsanov S. A, Klimov A.I., Korovin S. D., Kovalchuk B. M., Kurkan I. K., Loginov S. V., Pegel I. V., Polevin S. D., Volkov S. N., Zherlitsyn A. A., (2002), "S-Band Vircator with Electron Beam Premodulation Based on Compact Pulse Driver with Inductive Energy Storage", IEEE Transactions on Plasma Science, 30 (3),1179-1185.

[9] Chantrenne S., Bailey V. L., Goyer J. R., Putnam S. D., Riordan J. C., Steen P. G., Wilson A., (2003), "Bremsstrahlung Reflex Triode Modeling and Optimization", Titan Pulse Sciences Division.

[10] Chen X., Dickens J., Choi E. H., Mankowski J., Hatfield L. L., Kristiansen M., (2003), "Cavity Resonance Effect on a Coaxial Vircator", Center for Pulsed Power and Power Electronics, Department of Electrical and Computer Engineering and Physics, Texas Tech University.

[11] Chen X., Toh W. K., Lindsay P. A., (2003), "Improved Design of a Co-axial Virtual Cathode Oscillator", Dept. Of Electronic Engineering, University of London.

[12] Choi E. H., Sung K. Y., Jeon W., Chun S. H., Song K. B., Jung Y., Choi M. C., (2003), "Power Efficiency Enhancement of a Coaxial Virtual Cathode Oscillator with Ring-Type Reflector", Charged Particle Beam and Plasma Laboratory, Department Of Electrophysics/ Pulse Driven Power Research Center, Kwangwoon University.

[13] Song K. B., Sung K. Y., Jeon W., Jung Y., Choi M. C., Choi E. H., (2003), "The Diagnostics of High-Power Microwave From Virtual Cathode Oscillator with the Coupled Line Band Pass Filter", Charged Particle Beam and Plasma Laboratory, Department Of Electrophysics/ Pulse Driven Power Research Center, Kwangwoon University.

[14] Selemir V. D., Dubinov A. E., Ryaslov E. A., Kargin V. I., Efimova I. A., Loyko M. V., (2004), "A High-Power Vircator Operating as an X-ray Bremsstrahlung Generator", Plasma Physics Reports, vol. 30 (9), 772-778.

[15] Alekhin B. V., Voronin V. V., Voronov S. L., Kovalenko O. I., Pavlov S. S., Selemir V. D., Stepanov N. V., Suvorov V. G., Suryakov V. D., (2004), "Effective Pulsed-Repetitive Vircator with Double Anode Grid", Beams 2004, pp.544-547.

[16] Chen X., Dickens J., Mankowski J., Hatfield L. L., Choi E. H., Kristiansen M., (2004), "Microwave Frequency Determination Mechanisms in a Coaxial Vircator", IEEE Transactions on Plasma Science, 32 (5), 1799- 1804.

[17] Yang W., Ding W., (2004), "Studies on a New Dual- Coaxial Vircator", IEEE Transactions on Plasma Science, 32 (3), 1187-1190.

[18] Chen Y. J., (2005), " Compacti Repetitive Marx Generator and HPM Generation with the Vircator", Master Thesis, Texas Tech University.

[19] Lie L., Li-Min L., Xiao-Ping Z., Jian-Chun W., Hong W., (2006), "Pulse-Width Increase of Reflex Triode Vircator Using the Carbon Fibre Cathode", Chin. Phys. Lett., 23 (4), 899-902.

[20] Steinbauer M., Fiala P., Drexler P., (2006), "Measurement of Vircator Single-Shot High Power EM Pulse", Applied Electonics 2006, Pilsen 6-7 September 2006.

[21] Appelgren P., Akyuz M., Elfsberg M., Hurtig T., Larrson A., Nyholm S. E., Möller C., (2006), "Study of a Compact HPM System with a Reflex Triode and a Marx Generator", IEEE Transactions on Plasma Science, 34 (5), 1796-1805.

[22] Chupikov P. T., Faehl R. J., Onishchenko I. N., Prokopenko Y. V., Pushkarev S. S., (2006), "Vircator Efficiency Enhancement Assisted by Plasma", IEEE Transactions on Plasma Science, 34 (1), 14-17.

[23] Chen Y., Mankowski J., Walter J., Kristiansen M., (2007), " Cathode and Anode Optimization in a Virtual Cathode Oscillator", IEEE Transactions on Dielectrics and Electrical Insulation, 14 (4), 1037-1044.

[24] Dubinov A. E., Efimova I. A., Kargin V. I., Ryaslov E. A., Selemir V. D., (2007), "Generation of Soft X Rays in a Vircator with Exploeding Anode Foil, ISSN 1063-7842, Technical Physics, 52 (6), 809-811.

[25] Weber B. V., Commisso R. J., Coopersteing G., Hinshelwood D. D., Mosher D., Murphy D. P., Stephanakis S. J., Swanekamp S. B., (2007), "Reflex Triode X-Ray Source Research on Gamble II", Plasma Physics Division, Naval Research Laboratory, Washington, USA.

[26] Zhang Y., Ling Y., (2008), "Influence of Anode Plasma on High-Power Microwave Generation in Virtual Cathode Oscillator", Department of Engineering Physics, Tsinghua University.

[27] Kalinin Yu. A., Rempen I. S., Hramov A. E., (2008), "Numerical and Experimental Study of Controlling Characteristics of Generation in Low-Voltage Vircator by External Harmonical Signal", Saratov State University.

[28] Drazan L., Vrana R., (2009), "Axial Vircator for Electronic Warfare Applications", RADIOENGINEERING, 18 (4), 618-625.

[29] Polevin S. D., Kurkan I. K., Tsygankov R. V., (2009), "S-Band Coaxial Vircator with Electron Beam Premodulation", Instute of High Current Electronics SB RAS.

[30] Akafyeva N. A., Miroshnichenko A. Yu, Tsarev V. A., Biryukov I. S., (2010), "Experimental Investigation of a Low-Voltage Vircator with Preliminary Modulation of a Electron Beam", Saratov State Technical University.

[31] Song K. B., Byeon Y. S., Choi E. H., (2010), "Output Characteristics of the High Power Microwave Generated from an Axial and Triode Virtual Cathode Oscillator", Charged Particle Beam and Plasma Laboratory Pulse Driven Power Research Center, Kwangwoon University.

[32] Tsygankov R. V., Kitsanov S. A., Kovalchuk B. M., Polevin S. D., Suhov M. Y., Zherlitsyn A. A., (2010), "S-Band Coaxial Vircator with Electron Beam Premodulation Based on Compact LTD", High Power Microwaves 2010.

[33] Becker E. C., (2011), "Design and Simulation of a Compact Radiating System for High Power Microwaves in the 4 to 6 GHz Range", Master Thesis, University of Missouri Colombia.

[34] Kalinin Y. A., Stardubov A. V., Fokin A. S., (2011), "Experimental Study of the Scenario of Transition to Broadband Oscillations in Low-Voltage Vircator", 21st Int. Crimean Conference "Microwave & Telecommunication Technology" (CriMiCo' 2011), 12- 16 September, Sevastopol, Ukraine.

[35] Parson J. M, (2012), "Gas Evolution, Conditioning, and Electron Emission Properties of Carbon Fiber Cathodes in a Sealed Reflex- Triode Vircator", Doctoral Thesis, Texas Tech University.

[36] Phrolov N. S., Kalinin Y. A., Koronovskiy A. A., (2012), "The Increase of Output Microwave Power of a Vircator by Means of External Weak Single-Frequency Signal Influence", 22nd Int. Crimean Conference "Microwave & Telecommunication Technology" (CriMiCo' 2012), 10- 14 September, Sevastopol, Ukraine.

[37] Clements K. R., Curry R. D., Druce R., Carter W., Kovac M., (2013), "Design and Operation of a Dual Vircator HPM Source", IEEE Transactions on Dielectrics and Electrical Insulation, 20 (4), 1085-1092.

[38] Taylor M., Kelly P., Lynn C., Parson J., Mankowski J., Neuber A., Dickens J., Kristiansen M., (2013), "Frequency Tunable Sealed Tube Reflex Triode Vircator", Center for Pulsed Power and Power Electronics, Texas Tech University.

[39] Dubinov E. A., Tarakanov V. P., (2016), "PIC Simulation of the Dynamics of Electrons in a Conical Vircator", IEEE Transactions on Plasma Science, 44 (8), 1391-1395.

[40] Lynn C., Barnett D., Rainwater K., Neuber A., Dickens J., Mankowski J., (2016), "Reflex Triode Vircator Design for Extended Frequency Tuning Capabilities", Power and Power Electronics Dept. of Electrical and Computer Engineering, Texas Tech University.

[41] Barnett D. H., Rainwater K., Dickens J. C., Neuber A. A., Mankowski J. J., (2017), "Results of a Compact Reflex Triode with Multi Cavity Adjustment", Dept. of Electrical and Computer Engineering, Texas Tech University.

[42] Benford J., Swegle J. A., Schamiloglu E, (2016), "High Power Microwaves", 5th Edition, CRC Press.

[43] Benford J., Swegle J. A., Schamiloglu E, (2006), "High Power Microwaves", 2nd Edition, Taylor & Francis Group.

[44] Champeaux S., Gouard Ph., Cousin R., Larour J., (2016), "Improved Desing of a Multistage Axial Vircator With Reflectors for Enhanced Performances", IEEE Transactions on Plasma Science, 44 (1), 31-38.

[45] Fuks M.I., Prasad S., Schamiloglu E., (2016), "Efficient Magnetron With a Virtual Cathode", IEEE Transactions on Plasma Science, 44 (8), 1298-1302.

[46] Web 1, (2013), https://www.researchgate.net/publication/224722657, (Date of Acces: December 28, 2013)

[47] Web 2, (2015), https://www.researchgate.net/publication/264424971, (Date of Acces: November 20, 2015).

[48] Web 3, (2011), https://aip.scitation.org/doi/10.1063/1.3646361, (Date of Acces: September 7, 2011).

BIOGRAPHY

Hasan ERCIYAS was born in 1987 in Istanbul. He successfully completed the Physics Department of the Institute of Science and Technology at Gebze Technical University. He started his graduate studies at Gebze Technical University, Institute of Science, Department of Physics, Metrology Program. Since 2015, he has been working as a researcher at the Cathode and Microwave Vacuum Tube Research Center within TUBITAK BILGEM.